CHAPTER 5

PETROLOGY OF FELSIC GRANULITES

This chapter focuses on the collection and examination of three primary types of felsic granulite samples from the EGP. Specifically, these sample types consist of charnockite, granites, and monzosyenites. The subsequent sections provide comprehensive description of each of these samples.

5.1 Charnockite

5.1.1 Petrography

The massif-type charnockite from EGP exhibits a remarkable similarity in its mineralogy and texture. However, there are some differences between the samples. This specific rock has experienced high-grade metamorphism and preserves evidence of cooling from its peak metamorphic pressure-temperature conditions. Additionally, it shows signs of intense recrystallization during ductile shearing, while some parts still retain remnants of its original magmatic textures. Table 5.1 shows the location and broad description of all the charnockite samples used in the study.

The majority of the samples in the study area show porphyritic texture, featuring a coarse-grained granoblastic fabric and containing lath-shaped feldspar (both K-feldspar and plagioclase). All the feldspar grains preserve relict igneous textures like primary twinning. The broad mineralogical association of the charnockite consists of orthopyroxene (Opx) + plagioclase (Pl) + K-feldspar (Kfs) + quartz (Qtz) + ilmenite (Ilm) + apatite (Ap) + biotite (Bt) ± garnet (Gt) ± magnetite (Mt) ± Clinopyroxene (Cpx) + zircon (Zrn) ± pyrrhotite (Po) ± chalcopyrite (Cp). The rocks have been categorized into two groups, one with garnet in the assemblage and the other without it.

The charnockite containing garnet (Grt-bearing charnockite) exhibits both textural and mineralogical differences. This rock displays a coarse granoblastic texture, comprising quartz, K-feldspar, plagioclase, orthopyroxene, and ilmenite in addition to garnet porphyroblasts (Grt_1). Biotite is present as a secondary mineral, and occasionally hornblende (Hbl) has also been found. As accessory minerals, there are zircon (Zrn), apatite (Ap), pyrrhotite (Po), and chalcopyrite (Cp). Furthermore, one sample (PLB89A) contains clinopyroxene (Cpx) as a porphyroblastic phase along with other minerals. The rock contains a relatively low abundance of orthopyroxene, comprising less than 20% of its mineral composition. Interestingly, the distribution of

orthopyroxene within the rock exhibits a distinct bimodal pattern. The common occurrence of orthopyroxene is porphyroblastic, subhedral and elliptical in shape, while the other type is finer and has undergone recrystallization. In the majority of cases, these porphyroblasts exhibit a range of deformational characteristics. Notably, they tend to align preferentially along the foliation planes, often adopting a spindle-shaped geometry. There is evidence of marginal recrystallization, where the porphyroblasts transform into smaller, strain-free granules. Subgrain formation is also observed in these porphyroblasts. In some instances, the elliptical orthopyroxene shows localized patches of biotite development, often accompanied by occasional occurrences of iron oxide along the cleavage and fracture planes (Fig. 5.1). Orthopyroxene is found alongside garnet porphyroblasts, but without any apparent reaction relationship. In certain areas, coarse orthopyroxene grains are surrounded by a spongy intergrowth of garnet-quartz (Fig. 5.2). Some of the samples exhibit a noticeable gneissic foliation, as indicated in Table 5.1, while others appear massive or possess a less distinct foliation pattern. In the foliated samples, the gneissic foliation is characterized by alternating layers of orthopyroxene + garnet-bearing and quartzofeldspathic layers. Garnet occurs as porphyroblastic phase (referred to as Grt_1) containing inclusion of quartz, biotite and ilmenite, often surrounded by a thin collar of quartz (Fig. 5.3) and K-feldspar. Garnet also occurs in finer matrix grains (referred to as Grt_2), forming partial corona on ilmenite and orthopyroxene (Fig. 5.4). A double corona consisting of quartz and finer matrix garnet (Grt_2) has also formed around coarse orthopyroxene (Fig. 5.5). In some instances, biotite partially replaces orthopyroxene and garnet, while hornblende partially replaces clinopyroxene in a single sample (Fig. 5.6). Symplectic intergrowths between K-feldspar and ilmenite occur at the peripheries of biotite grains (Fig. 5.7), but this texture is rather sporadic in occurrence. Plagioclase porphyroblasts show antiperthitic texture, featuring irregular blebs and patches of K-feldspar (Fig. 5.8). Within the coarse perthite grains, there is a varying amount of exsolved plagioclase. In some cases, the proportion of exsolved phases is significant enough to classify the phase as mesoperthite. The exsolved plagioclase exhibits diverse sizes and shapes, including lamellar, bead-like, rod-like, and patchy structures. Moreover, perthitic K-feldspar grains contain pockets of quartz (Fig. 5.9) and commonly replaced by myrmekitic intergrowth of plagioclase and quartz along the grain boundaries. Two distinct sizes of myrmekitic intergrowth between quartz and plagioclase have been observed, with one appearing coarse and the other appearing fine (Fig. 5.10). The proportion of plagioclase and K-feldspar varies among the different samples. Additionally, some matrix quartz

and feldspar grains display cuspate grain boundaries. Deformation features are observable in the majority of grains, such as quartz, orthopyroxene, and feldspar, which exhibit undulose extinction, dynamic recrystallization, and subgrain formation. At places, xenoblastic quartz grains shows chessboard twinning, while the plagioclase grains show tapering twin edges. Notably, in a sample collected from the Ranipathar shear zone (sample PLB7/2), all phases display evidence of stretching along the foliation direction.

Charnockite lacking garnet (Grt-absent charnockites) exhibits overall comparable field relationships and texture to the charnockite that contains garnet (Grt-bearing charnockite). However, certain Grt-absent rocks show distinctive field relationships, such as an orbicular structure (Fig. 3.19). This structure consists of megacrystic plagioclase grains, reaching sizes of up to 6 cm in length, embedded within an orthopyroxene-plagioclase-quartz matrix. Porphyroblastic orthopyroxene grains are replaced by an intergrowth of biotite and quartz (Fig. 5.11). The presence of cuspate grain boundaries between quartz and feldspar grains (Fig. 5.12) suggests the possibility of crystallization from of a melt.

The rock provides compelling evidence of deformation. The occurrence of quartz ribbons, recrystallized nature of quartz, feldspars, and orthopyroxene, deformation twinning in plagioclase and kink bands in biotite are common feature.

5.1.2 Mineral chemistry

Table 5.2 presents spot chemical data, revealing a substantial variation in minerals among the samples. Compositional differences are evident within phases of individual samples, while minerals also exhibit chemical zoning, as described below.

Garnet exhibits X_{Mg} [=Mg/ (Mg + Fe^{2+})] variations ranging from 0.11 to 0.36. The primary compositional differences are observed in the almandine, pyrope, and grossular components. The spessartine component is consistently low, accounting for less than 3 mol% in all analyses, while uvarovite and andradite components are negligible, making up less than 1 mol%. The composition ranges from narrow ($Alm_{65–67}$ $Prp_{13–14}$ $Grs_{16–18}$) to broader ($Alm_{66–76}$ $Prp_{9–14}$ $Grs_{7–22}$) within different samples. Grt_2 is richer in Fe, displaying compositional variations in terms of Mg-Ca, ranging from ($Alm_{64–72}$ $Prp_{8–25}$ $Grs_{6–21}$).

Orthopyroxene exhibits compositional variations in terms of X_{Mg}, ranging from 0.42 to 0.59 across different samples. The Al_2O_3 content is generally low, staying below 2 wt.%, except for

sample 17EG18B, where it reaches up to 4.78 wt.%. All phases show minimal Cr content, with Cr_2O_3 being less than 0.05 wt.%, and the stoichiometrically recalculated Fe^{3+} content is also low, remaining below 3.0 wt.%.

Biotite exhibits compositional variations in terms of X_{Mg}, ranging from 0.40 to 0.87 across various samples. Regardless of their textural mode, all phases show variable TiO_2 content (3–6 wt.%) and F content (2–4 wt.%).

Plagioclase contains a minimal orthoclase component, accounting for less than 3 mol%. However, the anorthite and albite components vary among samples, ranging from $An_{47–63}$ $Ab_{37–51}$ to $An_{30–49}$ $Ab_{50–70}$. On the other hand, K-feldspar exhibits significant compositional variation in terms of orthoclase and albite components across different samples, varying from $Or_{96–97}$ $Ab_{3–4}$ to $Or_{77–81}$ $Ab_{19–23}$.

Clinopyroxene display variations in Fe-Mg ratios (X_{Mg} = 0.51–0.64) and Al_2O_3 contents (0.79–2.75 wt.%). When in contact with Garnet, the phase shows a lower X_{Mg} value (0.51), but when in contact with Hornblende, the X_{Mg} value is higher (0.64). All phases display low Na content (Na2O < 0.5 wt.%), while the recalculated Fe^{3+} content varies between 2.8 and 4.0 wt.%.

Hornblende grains exhibit moderate TiO_2 content, ranging from 1.78 to 2.07 wt.%, and there is a slight variation in the distribution of Fe and Mg (X_{Mg} = 0.42–0.46). All compositions show negligible F content, with values below 0.05 wt.%. Based on Leake et al.'s classification (1997), these grains are classified as ferro-tschermakite to tschermakite in composition. Ilmenite contains small but variable amounts of hematite and geikielite components.

5.1.3 Metamorphic reactions

The field and petrographic features of the charnockite, such as the presence of feldspar megacrysts, inclusion-free porphyroblastic garnet, and preserved igneous textures involving orthopyroxene and clinopyroxene, strongly indicate its magmatic origin. The mineral assemblage comprising Opx + Pl + Kfs + Qtz ± Grt ± Cpx + Ap + Ilm + Zrn supports the fact that the rock was formed through magmatic crystallization.

The presence of varying mineral assemblages, such as Cpx dominating over Opx and the occurrence of garnet, among others, suggests that the magma experienced different degrees of differentiation as it cooled and solidified. This variability in mineral compositions is a result of

various processes during the formation and evolution of the charnockite. The textural data further support the idea that the peak metamorphic assemblage found in the charnockite is the same as the one formed during subsolidus cooling. This indicates that the rock retained its mineral composition even after experiencing metamorphic processes.

Deformation effects are evident in the charnockite, visible at both the rock-scale and grain-scale features. In certain samples, the porphyroblastic Opx and Ilm grains are surrounded by a symplectic corona of garnet (Grt_2) and quartz (Qtz), which separates these phases from plagioclase, which suggest the following reactions.

$Opx + Pl = Grt_2 + Qtz$ ……. (5.1)

$Ilm_{SS} + Pl + Qtz = Ilm + Grt_2 + O_2$ ……. (5.2)

Dasgupta et al. (1991) previously reported a reaction similar to the reaction (5.2) in mafic granulites from the EGP. Both reactions imply a cooling process from high temperatures along a near-isobaric cooling path.

The occurrence of Bt + Qtz symplectite surrounding porphyroblastic Opx and Grt grains implies the occurrence of the following reactions.

$Grt_1 + Opx + Kfs + melt = Bt + Qtz$ ……. (5.3)

$Opx + Kfs + melt = Bt + Qtz$ ……. (5.4)

Reactions (3 and 4) may take place during the cooling process in the presence of fluid or melt.

Sample PLB89A retains evidence of incipient melting of the matrix Bt. The Ti-rich Bt, in the presence of Qtz, reacted to create a symplectite composed of Kfs and Ilm along the margin, likely formed through the following reaction.

$Ti\text{-}Bt + Qtz = Kfs + Ilm + melt$ ……. (5.5)

It is important to note that this particular type of reaction typically occurs during a heating phase along a prograde path. This observation could potentially indicate a granulite facies reworking of the previously cooled crust.

5.1.4 Geothermobarometry

The pressure and temperature of metamorphism for the samples have been calculated using conventional geothermobarometers. Suitable mineral assemblages such as garnet-orthopyroxene-plagioclase-quartz, garnet-clinopyroxene, garnet-ilmenite, orthopyroxene-ilmenite, and garnet-biotite have been utilized to estimate both the temperature and pressure of equilibration for the

peak and post-peak assemblages (Table 5.3). Temperature in the range of 722–790°C is obtained using the garnet-orthopyroxene thermometer developed by Lee and Ganguly (1988) under an assumed pressure of 8 kbar. For various samples, the garnet-orthopyroxene-plagioclase-quartz thermobarometer proposed by Pattison et al. (2003) provides pressure estimates within the range of 7.30–9.03 kbar and temperature estimates spanning 741–910°C. Utilizing the garnet-ilmenite thermometer based on Pownceby et al. (1987) results in temperature estimates of 563–672°C. Temperature readings from Henry et al. (2005)'s Ti-in biotite thermometer fall between 756 and 831°C. On the other hand, Ganguly et al. (1996)'s garnet-biotite thermometer produces readings between 421 and 781°C. The trace element thermometry of Ti-in zircon, following the approach of Ferry and Watson (2007), has also been applied. Ti values have been obtained from the identical locations used for calculating U-Pb dates (Fig. 7.1). Temperatures of zircon crystallization (characterized by oscillatory zoning) and metamorphism (evident through overgrowth and patches) have been determined from the zircon domains. The calculated crystallization temperatures for various samples span the range of 660–862°C. Metamorphic temperatures, determined through Ti contents in zircon overgrowths and patches, exhibit variations within the range of 635–812°C.

Employing various conventional geothermometers, the analyses yielded maximum estimated values for temperature (T) and pressure (P) reaching up to 910°C and 9 kbar, respectively. These estimations are suggestive of the peak metamorphic phase, during which garnet and orthopyroxene were concurrently present alongside plagioclase and quartz. The lower temperature estimates, extending to approximately 420°C, potentially signify the subsequent post-peak metamorphic phase, marked by Fe-Mg re-equilibration between garnet and biotite. This process reflects a phase of mineral alteration and resetting in the rock's history. The temperatures deduced for both crystallization and metamorphism, based on zircon's titanium content, exhibit a substantial degree of convergence. Nevertheless, it's important to recognize that these values should be regarded as conservative or minimal estimations, primarily due to the presence of ilmenite as the phase that reaches titanium saturation within the system (Watson et al., 2006 and Ferry and Watson, 2007). According to the computations by Ferry and Watson (2007), the genuine temperatures under these circumstances would likely be elevated by approximately 70°C compared to the inferred values. This adjustment factors in the impact of the titanium-saturating

phase and underscores the potential for the actual temperatures to be notably higher than initially estimated.

5.1.5 Whole rock chemistry

The compositions of the chosen samples are displayed in Table 5.4, detailing the major, trace, and rare earth elements. All the samples exhibit elevated levels of TiO_2, Al_2O_3, CaO, total Fe (FeO_T), and Mg# (excluding the PLB89A sample). The SiO_2 content shows considerable variability, leading to the categorization of samples into high-SiO_2 and low-SiO_2 types. Samples having SiO_2 content between 53-62 wt.% are within low SiO_2 group and those within 63-72 wt.%, belongs to high SiO_2 group. While Al_2O_3 content in all the samples remains modest (<15 wt.%), there is a broad range of variation in FeO_T (3.07–11.07 wt.%) and MgO (0.56–8.35 wt.%). The composition of CaO (ranging from 2.81 to 5.8 wt.%) and K_2O (ranging from 1.36 to 5.14 wt.%) also demonstrates significant variability. Calculated LOI values are less than 1 wt.%, indicating the dry nature of the mineral combinations. Numerous major and trace element diagrams reveal a negative correlation between SiO_2 with TiO_2, P_2O_5, FeO_T, CaO, Al_2O_3, Sr, Zr, Ce, Y, and Mg, while showing a positive correlation with Ba and Ni. While characterizing the evolution and paleotectonic setting of the charnockite magma using geochemical proxies, the major elements have been avoided due to their higher likelihood of mobilization during high temperature metamorphism and recrystallization. Plots involving trace and rare earth elements have been utilized for their greater reliability.

In the classification diagram of total alkali vs SiO_2 (TAS) (Fig. 5.13), the fields ranging from gabbroic diorite to diorite accommodate the low-SiO_2 samples, while the granodiorite to granite fields contain the high-SiO_2 samples. The feldspar An-Ab-Or diagram positions the samples within the tonalitic to quartz monzonite fields (Fig. 5.14). These patterns exhibit notable resemblance to the charnockites found in the Mawson Coast (MC) and the Northern Prince Charles Mountains (nPCM) regions of East Antarctica. The SiO_2-Fe* plot, after Frost and Frost (2008), illustrates that the samples represent an intermediate category, encompassing characteristics of both the ferroan and magnesian groups (Fig. 5.15). This positioning partially coincides with the charnockites of the MC and nPCM regions (Frost and Frost 2008; Rajesh 2007; Rajesh and Santosh 2004). The samples exhibit overlapping distribution between the I- and S-type granitoids, much like the other intermediate charnockites do (Fig. 5.16). According to Frost et al. (2001)'s modified

alkaline-lime index (MALI) plot, the samples from the high-SiO_2 group are mostly calcic- to calc-alkalic, whereas those from the low-SiO_2 group are calc-alkalic to alkali-calcic (Fig. 5.17). In the ASI vs A/NK plot, the samples exhibit peraluminous to metaluminous attributes (Fig. 5.18). Regarding the Th vs Co plot introduced by Hastie et al. (2007), the majority of samples demonstrate compositions ranging from high-K calc-alkaline to shoshonite (Fig. 5.19). None of the samples display affinities with TTG/adakite when presented on Martin's (1986) Yb_N vs La_N/Yb_N binary diagram (Fig. 5.20). The extended trace element plot, normalized to MORB values using the methodology of Sun and McDonough (1989), demonstrates an enrichment in Rb, Th, K, Nd, Zr, and Hf, while exhibiting depletion in Nb, Sr, Ta, P, and Ti (Fig. 5.21). On the Rb-Ba-Sr ternary plot, the samples share similarities with low Ba-Sr granitoids, with the exception of three samples (PLB24, 19EG06, PLB2B) that display affinities towards high Ba-Sr granitoids (Fig. 5.22). All samples have elevated Y content (ranging from 7 to 82.3 ppm, average of 37.63 ppm) and varying but generally modest levels of Sr content (ranging from 57 to 222 ppm, average of 146.76 ppm), which results in low Sr/Y ratios (ranging from 1.34 to 31.67, average of 7.20). Three samples, PLB82A, 19EG06, and PLB71B, however, have Y concentrations that are noticeably lower (between 7 and 9 ppm), which results in greater Sr/Y ratios. In contrast to the other samples, these particular samples exhibited unique behavior on the Sr/Y vs. Y plot, showing an affinity more in line with Archean high-Al TTG (Tonalite-Trondhjemite-Granodiorite) compositions (Fig.5.23). The majority of samples exhibit Rb/Sr ratios exceeding the mantle value of 0.03 (Fig. 5.24), signifying characteristics associated with the upper crust. The samples' La/Th vs. Th/U diagrams marginally diverge from the range of typical igneous rocks (Fig. 5.25), which may suggest that the rocks underwent a U-depletion process during metamorphism with comparatively little Th-depletion. The high- and low-SiO_2 charnockite varieties infer a collisional setting based on the Nb/Zr vs Zr plot (Fig. 5.26) created by Thieblemont and Tegyey (1994). The bulk of samples fit with the features of an alkaline arc setting using the Hollocher et al. (2012) La/Yb vs Nb/La plot (Fig. 5.27).

Following McDonough and Sun (1995), the primitive mantle-normalized REE plot exhibits highly fractionated patterns that are distinguished by enrichment of LREE relative to HREE (Fig. 5.28). Additionally, high La/Yb_{CN} (1.54–9.68; average 5.0) is indicative of this. Conversely, the fractionation of HREE presents a nearly uniform trend, with Ta/Yb_{CN} values indicating depletion, ranging from 1.05 to 1.36, with an average of 1.18 for samples 17EG13,

17EG10, S26, and ranging from 1.5 to 3.6, with an average of 2.11 for the remaining samples. The prevailing feature among the samples is the presence of a negative Eu anomaly, with Eu/Eu* ratios ranging from 0.4 to 1.5, and an average of 0.66.

5.1.6 Phase equilibria analysis

To better understand the geological history of the coarse-grained charnockite before it underwent metamorphism, we conducted phase equilibria modeling within the pressure-temperature (P-T) range of 6-11 kbar and 600-1200°C. This modeling was performed using the software Perple_X 6.9.0 (Connolly, 2005, 2009). The working hypothesis is that under lower crustal conditions, magma derived from a suitable protolith crystallized to become charnockite. Experimental and natural occurrence data suggest that charnockite magma can be produced from hydrated basalt or dehydration melting of amphibolite protoliths at lower crustal conditions (Wendlandt, 1981; Rajesh et al., 2014; Grantham et al., 2012). Thus, a hydrated basaltic bulk composition from the neighboring East Dharwar Craton was chosen (Manikyamba et al., 2015) as the "suitable" protolith to test this theory for the current samples. The current data indicate that onset of melting occurs at temperatures exceeding 850°C under lower crustal pressure conditions (6-10 kbar). The graphical representation in Figure 5.29 demonstrates that approximately 23% of the bulk composition undergoes melting at around 1000°C and 8 kbar pressure, resulting in the formation of a melt phase with a composition resembling that of a granitic material. To comprehend the chemistry of the melt, melt compositions and modal volumes were calculated at two distinct temperatures (900°C and 1000°C) under a pressure of 8 kbar. The calculated melt compositions were subsequently depicted in various geochemical diagrams.

The findings reveal that at a temperature of 900°C and a pressure of 8 kbar the produced melt can account for as much as 11% and may consist of over 60 wt% SiO_2. Meanwhile, under the same initial composition, at 1000°C and 8 kbar pressure, the generated melt can reach up to 25% with a SiO_2 content ranging from 52% - 56% wt.% (Fig.5.29). All the extracted melt compositions were plotted in a TAS diagram for the purpose of comparison, revealing that at 900°C, the melt compositions are situated within the quartz monzonite field (Fig. 5.30a). On the other hand, those at 1000°C exhibit relatively higher Na_2O and K_2O contents, positioning them within the monzodiorite to monzonite fields (Fig. 5.30b). The calculated compositions do not align precisely with the chemistry of charnockite, as the latter is situated within the spectrum of gabbroic diorite to granite compositions (Fig.5.13). Nonetheless, the inferred melt and charnockite magma

compositions exhibit a comparable pattern in the TAS diagram, which may suggest the likelihood of some degree of crustal contamination influencing the magma.

5.1.7 Zircon trace element and REE chemistry

The trace and rare earth element (REE) concentrations of selected zircon grains from charnockite were assessed at the exact locations where U-Pb analyses were conducted. The collected data from eight samples are displayed in Table 5.5. Differences in the concentration levels of individual elements (measured in parts per million, ppm) have been observed both among various samples and within individual samples themselves. Among the sixty-five analyses conducted, fifty-three originated from the oscillatory-zoned zircon domain. To elucidate the geochemical context, a variety of bivariate and discrimination diagrams were employed, as outlined by Grimes et al. (2007, 2015). These diagrams serve as tools for interpreting the chemical composition and the likely environmental conditions associated with the samples.

The U/Yb versus Hf plots applied to magmatic zircon samples exhibit characteristic features reminiscent of continental arc signatures (Fig. 5.31a). These graphical representations provide insights into the elemental ratios of uranium (U) and ytterbium (Yb) relative to hafnium (Hf) within the zircon grains. Notably, the average U/Yb ratios observed in these zircons, which generally fall within the range of 0.1 to 4.0, further support their association with continental arc environments. Elevated U/Yb values within this range are indicative of potential contamination from mature, crustal components enriched in LILE elements (Grimes et al., 2015). The U/Nb versus Th/Nb plots (Fig. 5.31b) reveal pronounced elevated ratios, both surpassing critical thresholds (U/Nb > 20, Th/Nb > 10). These remarkable values provide strong indications of an arc-related geological context. In addition, the Nb/Yb versus U/Yb plot (Fig. 5.31c) show that a significant portion of the data points are positioned within the distinctive mantle zircon array. This particular array is recognized as a hallmark feature associated with magmatic arc environments. This observation aligns with the findings established by Grimes et al. (2015), reaffirming the interpretation of these zircons as originating from magmatic arcs. Ti vs Yb plots (Fig. 5.31d) and Ti vs Gd/Yb plots (Fig. 5.31e) were employed to gain insights into the crystal chemical mechanisms governing REE substitution within zircon. The role of amphibole in the crystallization of zircon is ruled out by the observed positive correlation between Yb and Ti (Fig.5.31d). On the other hand, the positive correlation between Ti and the Gd/Yb ratio (Fig. 5.31e) suggests the early separation of titanite

and apatite from the magma. The comparison between the compositions of the present zircon population and those with established provenance is depicted in Figure 5.32. This visual comparison provides valuable insights into the potential sources and formation conditions of the studied zircon samples, and it has been modified from the work of Grimes et al. (2015).

On the chondrite-normalized trace element discrimination plot, following the approach by McDonough and Sun (1995), the oscillatory-zoned zircon exhibits distinct characteristics. There are pronounced positive anomalies in U and Th, while negative anomalies are prominent in Eu and Ti (Fig. 5.31f). Additionally, relatively subtle positive anomalies are observed in Ce, Dy, and Sm, accompanied by modest negative anomalies in Pr and Nd. Both the chondrite-normalized and primitive mantle-normalized plots for rare earth elements (REE) (Fig. 5.31f and g) exhibit a clear pattern of light rare earth element (LREE) depletion and heavy rare earth element (HREE) enrichment. This distribution pattern is characteristic of igneous zircon formation within a granitoid magma context, aligning with previous findings (Hoskin and Black, 2002; Belousova et al., 2002). The trace element and REE patterns observed in the zircon overgrowth and patches exhibit substantial overlap with those seen in the magmatic zircons (Figure 5.31f and g). However, these patterns display further fractionation, with a slight reduction in LREE, a concave-up trend in HREE distribution spanning from Gd to Er, and a level distribution from Er to Lu. Notably, among the high field strength elements (HFSE), a distinct and strong negative anomaly is observed in the case of Ti.

5.2 Granite

5.2.1 Petrography

The studied granite samples are coarse grain, porphyritic, contains lath of both plagioclase and K-feldspar grains and have similar mineralogical assemblage and texture like the charnockite. The rock is generally composed of quartz (Qtz) + plagioclase (Pl) + K-feldspar (Kfs) ± garnet (Gt) + ilmenite (Ilm) + apatite (Ap) + biotite (Bt) ± sillimanite (Sil) along with accessory minerals such as Ap, Zrn, and Mnz. The details about their modal percentage and location are given in Table 5.1. Garnet occurs as idioblastic to sub-idioblastic, irregularly shaped porphroblastic phase, which contains numerous inclusions of Qtz, Bt, Ilm and Kfs. These porphyroblasts show symplectic overgrowth of Bt + Qtz along the margins (Fig. 5.33). Only one sample PLB 79 have bimordal distribution of garnet. Besides the porphyroblastic Gt_1, the rock also contains a fine grained, matrix

phase identified as Gt_2. Both plagioclase and K-feldspar preserve relict igneous texture. Perthite is very common. Often the large feldspar grains are altered to form sericite and they also preserve evidence of subgrain formation and recrystallization (Fig. 5.34). The matrix is composed of quartz, feldspar and biotite are locally recrystallized where the quarzofeldspathic matrix forming granoblastic texture. Additionally, they also show evidence of deformation like kinking in biotite grains, undulose extinction in quartz and feldspar grains and partial quartz ribbon formation. Cuspate grain boundary and intergrowth between plagioclase and quartz, forming myrmekitic texture along the grain boundary of porphyroblastic phase are common (Fig. 5.35). Notably, two sample (PH10 and 17EG15) contain micro-enclaves (Fig. 5.36) of aluminous granulite identified based on mineral assemblage like sillimanite + spinel + hemo-ilmenite grains. One sample (PH10) collected close to the Ranipathar Shear zone is highly deformed and mylonitized. The schistosity is defined by biotite, sillimanite and opaque phases are warped around the porphyroblastic grains, often forming symmetric-asymmetric tails (Fig. 5.37). Quartz ribbons are well developed here and the finely crushed, recrystallized matrix grains indicate mylonitization (Fig. 5.38). Additionally, the rock preserves well-developed gneissic banding where the melanocratic band is represented by association of garnet, biotite and opaque and the leucocratic band is represented by quartz, feldspar and sillimanite. Locally, thin film of quartz rim is observed around the plagioclase porphyroclast.

5.2.2 Whole rock geochemistry

Representative five sample has been chosen for geochemical analysis. The details of major, trace and REE data are given in Table 5.6. The granite shows a comparable geochemical composition to charnockite, with a wide range of SiO_2 (56.7-75.6 wt.%), FeO_T (0.98-7.95 wt.%), and MgO (0.07-1.9 wt.%). The one with low SiO_2 (sample PLB79) has higher Al_2O_3 (18.35 wt.%), TiO_2 (1.12 wt.%), Fe_2O_3 (7.08 wt.%) and CaO (3.68 wt.%) along with high concentration of trace like as (55 ppm), Ba (1105 ppm) and V (113 ppm) compared to other. The calculated value of LOI is less than 0.6 wt.%. ASI vs A/NK plot of Sand (1943) show that all the granites are of peraluminous character (Fig. 5.39). SiO_2 vs FeO_t plot show majority of sample belongs to ferroan group except one sample (Fig. 5.40). On the other hand, granite discrimination diagram SiO_2 vs ($Na_2O + K_2O – CaO$) MALI plot after Frost et al., (2001) the granites of EGP show broad range from calcic to alkali (Fig. 5.41). The total alkali vs silica (TAS) diagram after Middlemost (1994), majority of the data are plotted in the granitic field except one (sample PLB79) plot in the monzonite field (Fig. 5.42). The granites

generally show I and S type characteristic as confirmed from 1000*Ga/Al vs Zn plot (Fig. 5.43) after Whalen (1987). On the other hand, the extended trace element plot, normalized to MORB values using the methodology of Sun and McDonough (1989), show enrichment in Rb, Th, K, Pb and Li (except one) and depletion in Ba, Nb, Ta, Sr, P and Ti (Fig. 5.44). The Rb vs Y + Nb granite tectonic discrimination plot after Pearce et al., (1984) show overlapping characteristic between syn-collisional and within plate granite (Fig. 5.45). Additionally, the Nb/La vs La/Yb plot of Hollocher (2012) show arc signature which is similar to the charnockite reported in this study (Fig. 5.46). In accordance with the findings of McDonough and Sun (1995), the plot of rare earth elements (REE) normalized to the primitive mantle demonstrates distinctively fractionated patterns, characterized by notable enrichments of LREE and depletion of HREE. In the same diagram majority of the samples show negative Eu anomaly except one (PH10) which also show enriched trend for Gd, Tb, Dy, Ho and Er (Fig. 5.47).

5.3 Monzosyenite

The rock exhibits a finer-grained texture, primarily characterized by extensive recrystallization, and displays a predominantly greyish hue. The rock is composed of plagioclase + quartz + K-feldspar + biotite + ilmenite + zircon + monazite + allanite. Their modal abundance is given in Table 5.1. It is rich in plagioclase (Pl) and quartz (Qtz), with a comparatively infrequent occurrence of K-feldspar (Kfs). In certain areas, there are visible layers of biotite (Bt) flakes that display an incipient foliation. One significant aspect of the rock's composition is the distinctive occurrence of a layer rich in zircon (Zrn) and ilmenite (Ilm) (Fig. 5.48). Zircon is abundantly found within these layers, exhibiting a grain size ranging from 50 to 150 μm. Furthermore, alongside zircon, the zircon-ilmenite layer also contains the presence of monazite and allanite (Fig. 5.49). This layer seems to have formed as a result of the crystallization processes during the magmatic phase.

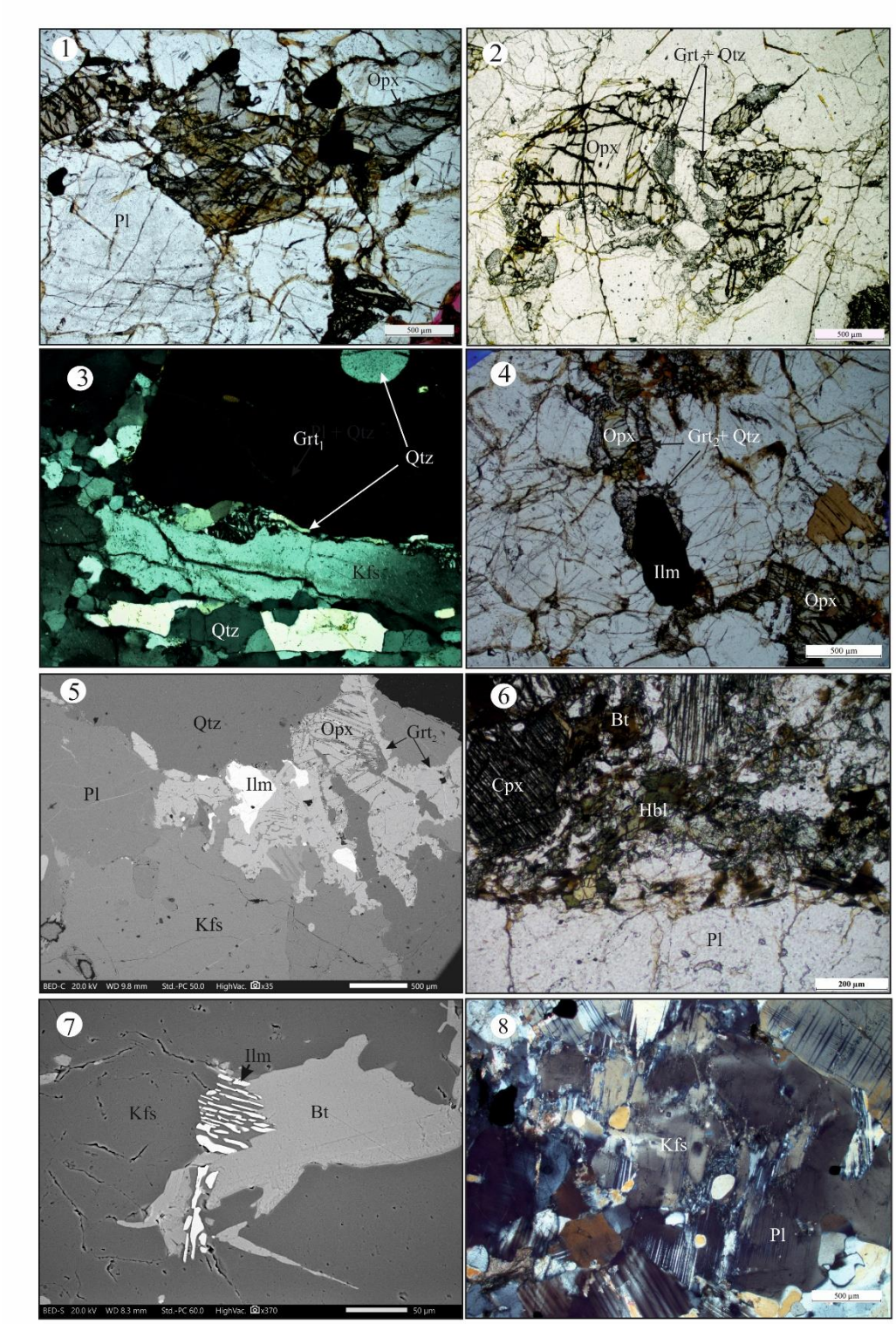

Fig. 5. Photomicrographs and Back- scattered electron (BSE) images of the massif type charnockite. (1) Iron oxide development along the fracture of orthopyroxene (Opx). (2) Spongy intergrowth of garnet and quartz (Qtz) along the margin of orthopyroxene. (3) Thin collar of quartz (Qtz) along the margin of porphyroblastic garnet (Grt_1) grains. (4) A double corona of intergrown garnet and quartz (Grt_2 + Qtz) surrounding porphyroblastic orthopyroxene (Opx) and ilmenite (Ilm). (5) Double corona of quartz (Qtz) and finer matrix garnet (Grt_2) around coarse orthopyroxene (Opx). (6) Porphyroblastic clinopyroxene (Cpx) showing replacement to hornblende (Hbl) and locally biotite (Bt). (7) Partial breakdown of biotite (Bt) to a skeletal intergrowth of K-feldspar and ilmenite (Kfs + Ilm). (8) Antiperthitic texture in plagioclase (Pl), showing irregular blebs and patches of K-feldspar (Kfs).

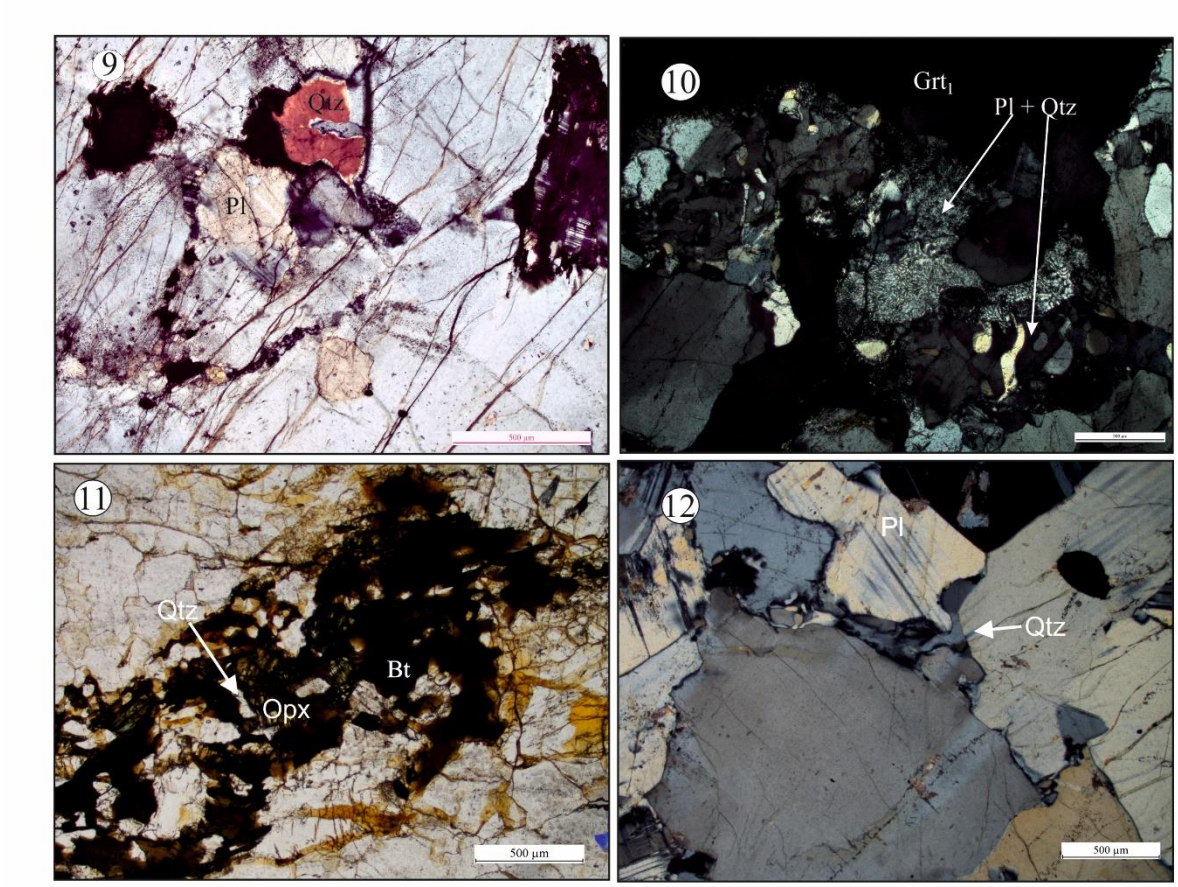

Fig. 5 (9) Oval inclusions of quartz (Qtz) and plagioclase (Pl) within coarse perthitic feldspar (Kfs). Note the occurrence of myrmekitic intergrowth along margins of Kfs. (10) Coarse and fine intergrowth of plagioclase (Pl) and quartz (Qtz). (11) Intergrowth of biotite (Bt) and quartz (Qtz) replacing the porphroblastic orthpyroxene (Opx). (12) Cuspate grain boundaries between quartz (Qtz) and plagioclase (Pl) grains.

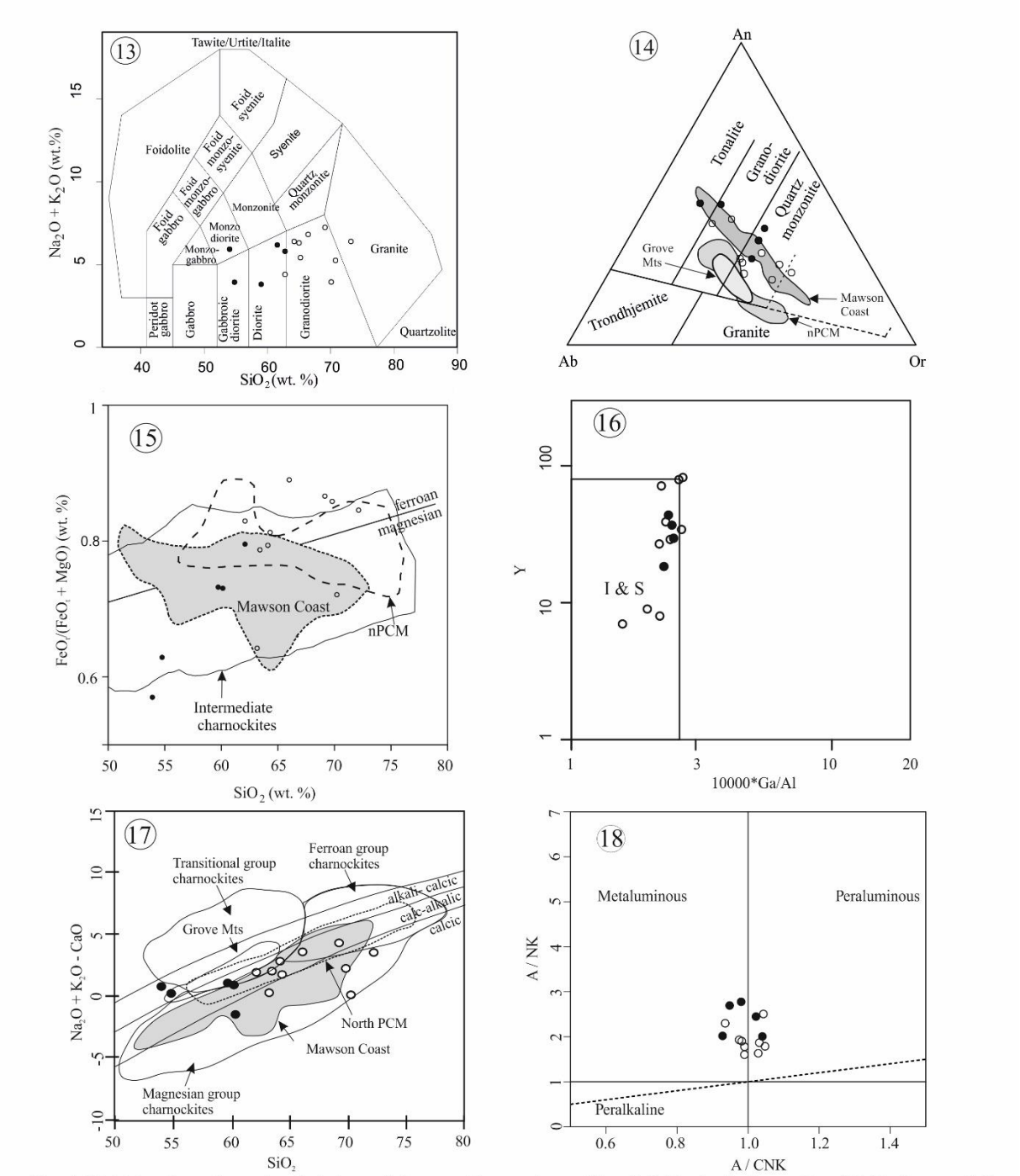

Fig. 5 Multiple plots of geochemical data of the massif type charnockite. (13) Total alkali vs silica (TAS) diagram (after Middlemost, 1994) plot of the samples. The filled circles represent the low-SiO_2 group and the open circles represent the high-SiO_2 group as described in the text. (14) An-Ab-Or triangular plot of the same samples. Fields showing charnockites from the northern Prince Charles Mountains (nPCM), Mawson Coast and Grove Mountains are shown after Sheraton et al. (1996), Zhao et al. (1997), Young et al. (1997), and Liu et al. (2009) are given for comparison. (15) SiO_2–Fe* plot (after Frost and Frost, 2008) of the same samples showing the similarity of the studied samples with the intermediate charnockites described by Rajesh and Santosh (2004). The other fields are same as (14). (16) Y vs. 1000* Ga/Al plot. (17) Modified alkaline -lime index (MALI) plot after Frost et al., (2001) show broad range from calcic to alkali-calcic. (18) A/CNK vs A/NK plot of the same samples. Note that the samples (both high- and low-SiO_2 groups) show metaluminous to weakly peraluminous characters.

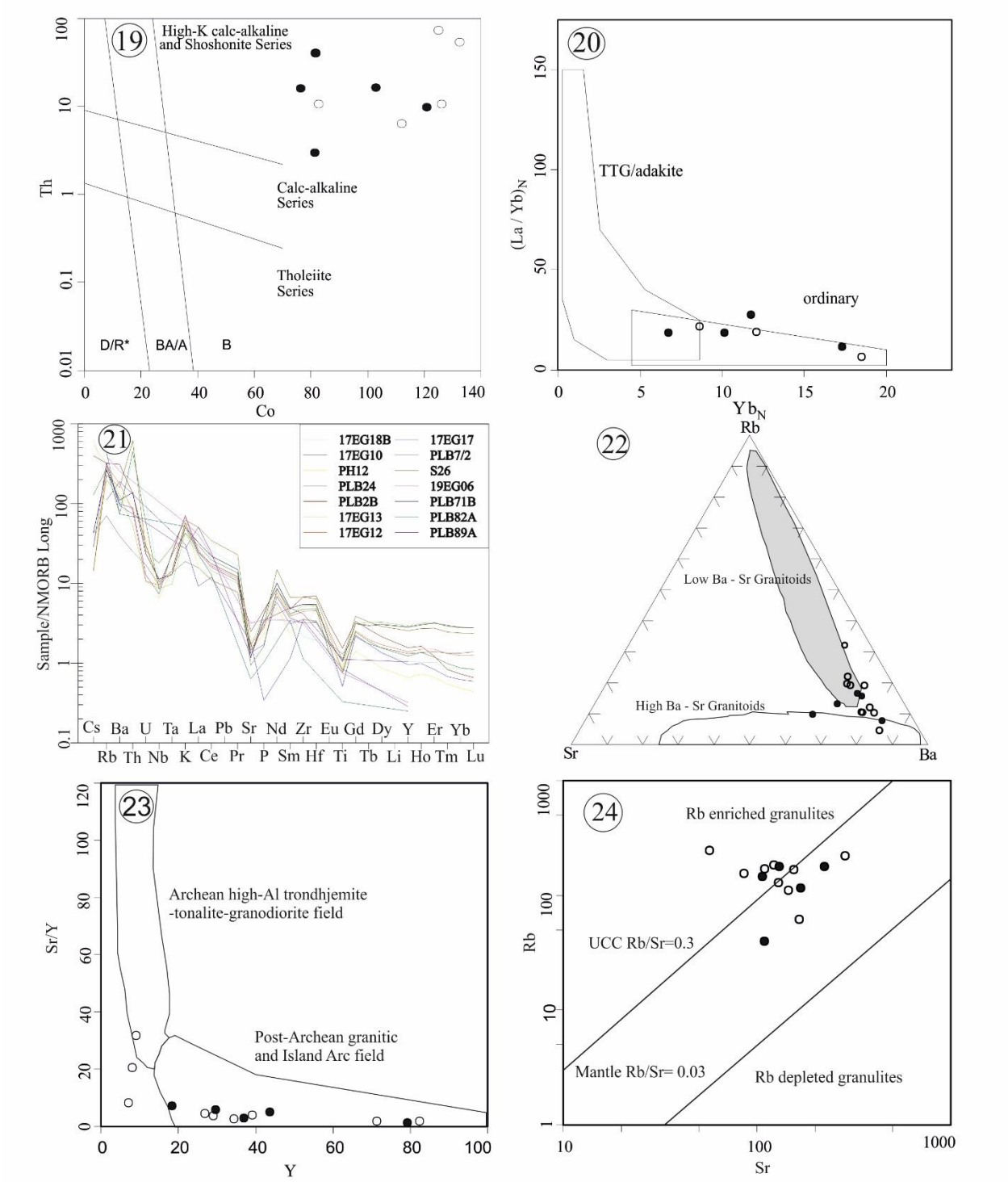

Fig. 5 (19) Th vs Co plot after Hastie et al. (2007). (20) YbN vs La_N/Yb_N binary plot of the same samples after Martin (1986). (21) Multi-element variation diagram for trace elements and REE of 14 samples normalized to MORB (after Sun and McDonough, 1989). Note the strong positive anomalies of Th, La, Ce and Nd while strong negative anomalies are found for Nb, P, Sr and Ti. (22) Triangular Rb-Ba-Sr plot. See Rajesh and Santosh (2004) for details on the fields. (23) Sr/Y vs. Y plot, the fields are from Drummond and Defant (1990). (24) Rb vs. Sr plot after Tomson et al., (2006)

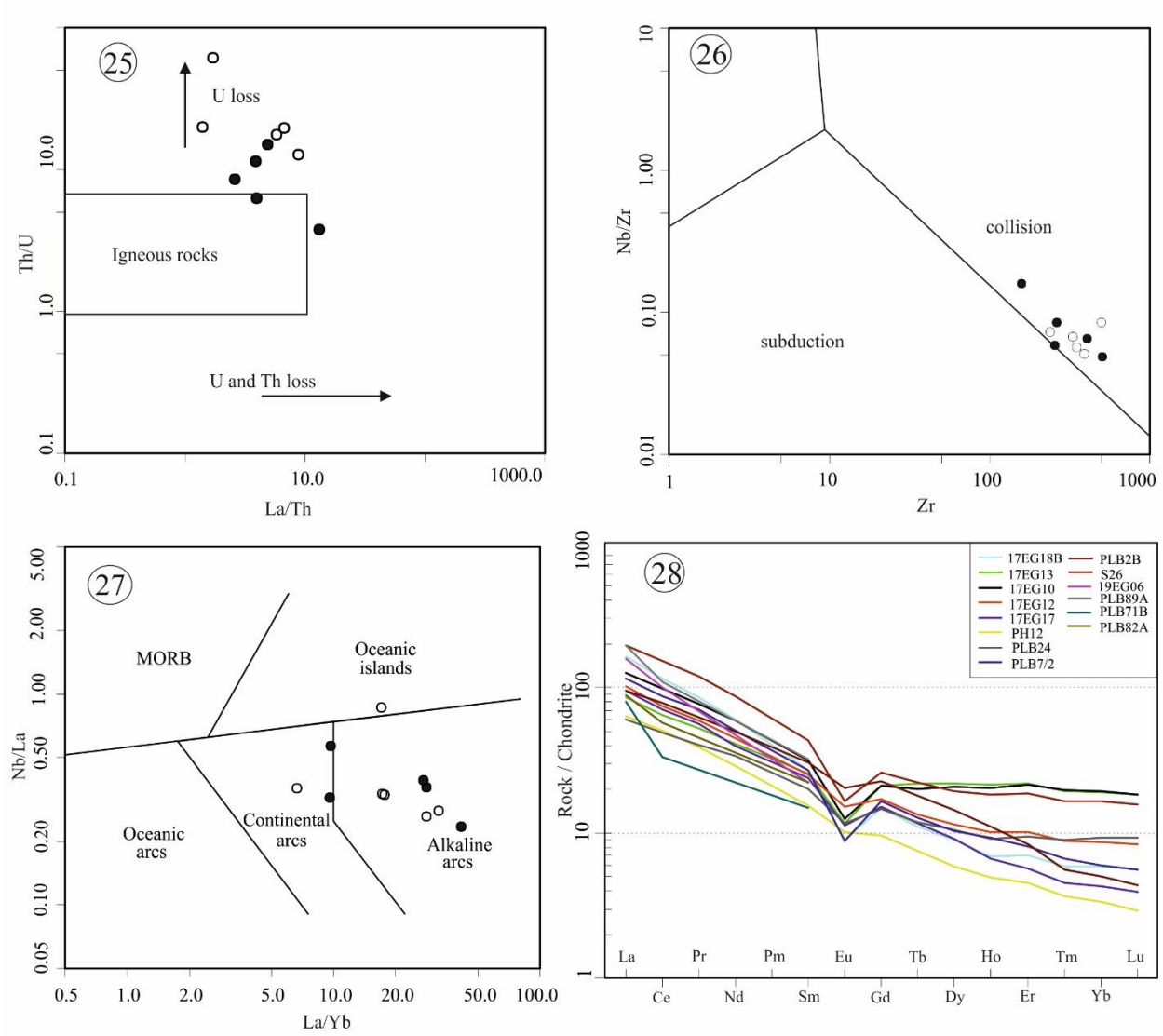

Fig. 5 (25) Th/U vs La/Th plot. Field of common igneous rocks are from Rudnick and Presper (1990). (26) log (Nb/Zr) vs. log Zr plot of the samples (the fields are from Thieblemont and Tegyey, 1994) showing all the samples plotting in the collision field. (27) Nb/La vs La/Yb plot of the same samples after Hollocher et al. (2012). Note the samples plot in the fields of alkaline arc to continental arc. (28) Chondrite-normalized REE plot (after McDonough and Sun, 1995) of the samples showing strongly fractionated REE patterns with a prominent negative Eu anomaly.

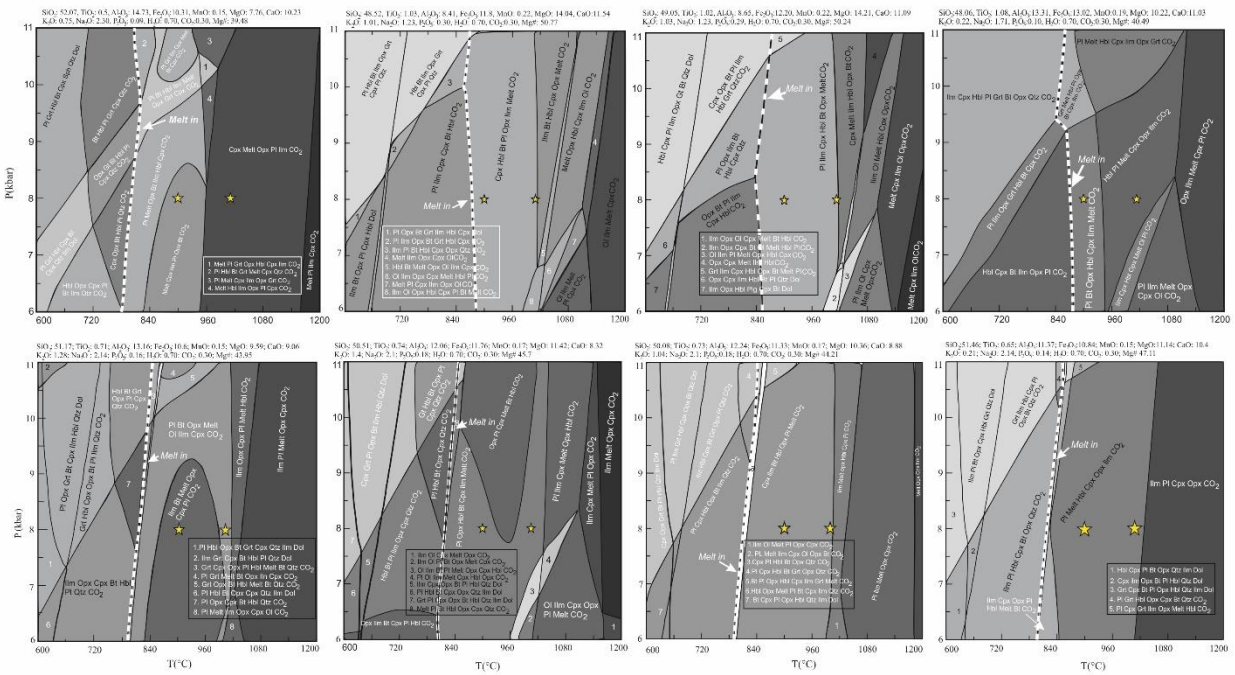

Fig. 5.29 Calculated phase diagram in the system Na_2O-CaO-K_2O-FeO-MgO-Al_2O_3-SiO_2-H_2O-TiO_2 for a representative bulk composition of hydrated basalt (Manikyamba et al., 2015). The phase diagram has been constructed at 0.30 wt% CO_2 and 0.70 wt% of H_2O. The diagram has been constructed using the program Perple_X (see text for details). Note the position of the "melt-in" curve in the system. The two asterisks marked represent the P-T conditions from which the melt compositions have been recalculated (see text).

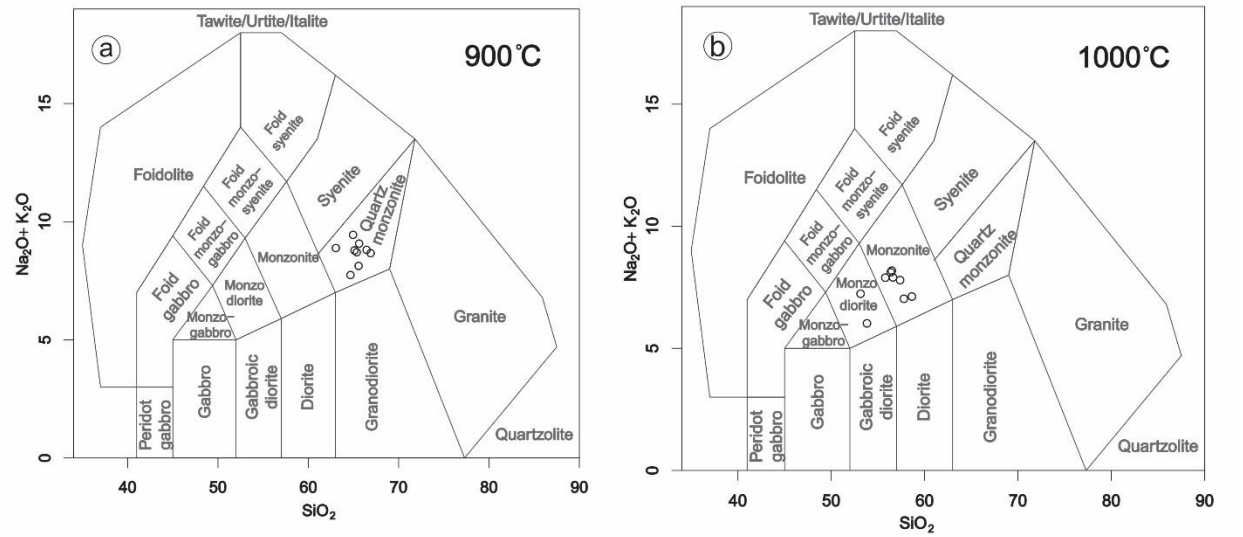

Fig. 5.30 (a and b) TAS diagram (after Middlemost, 1994) showing calculated melt compositions (a) at 900 ◦C, 8 kbar, and (b) 1000 ◦C, 8 kbar. Note that the compositions plot in the quartz-monzonite and monzonite-monzodiorite fields at 900 ◦C and 1000 ◦C, respectively.

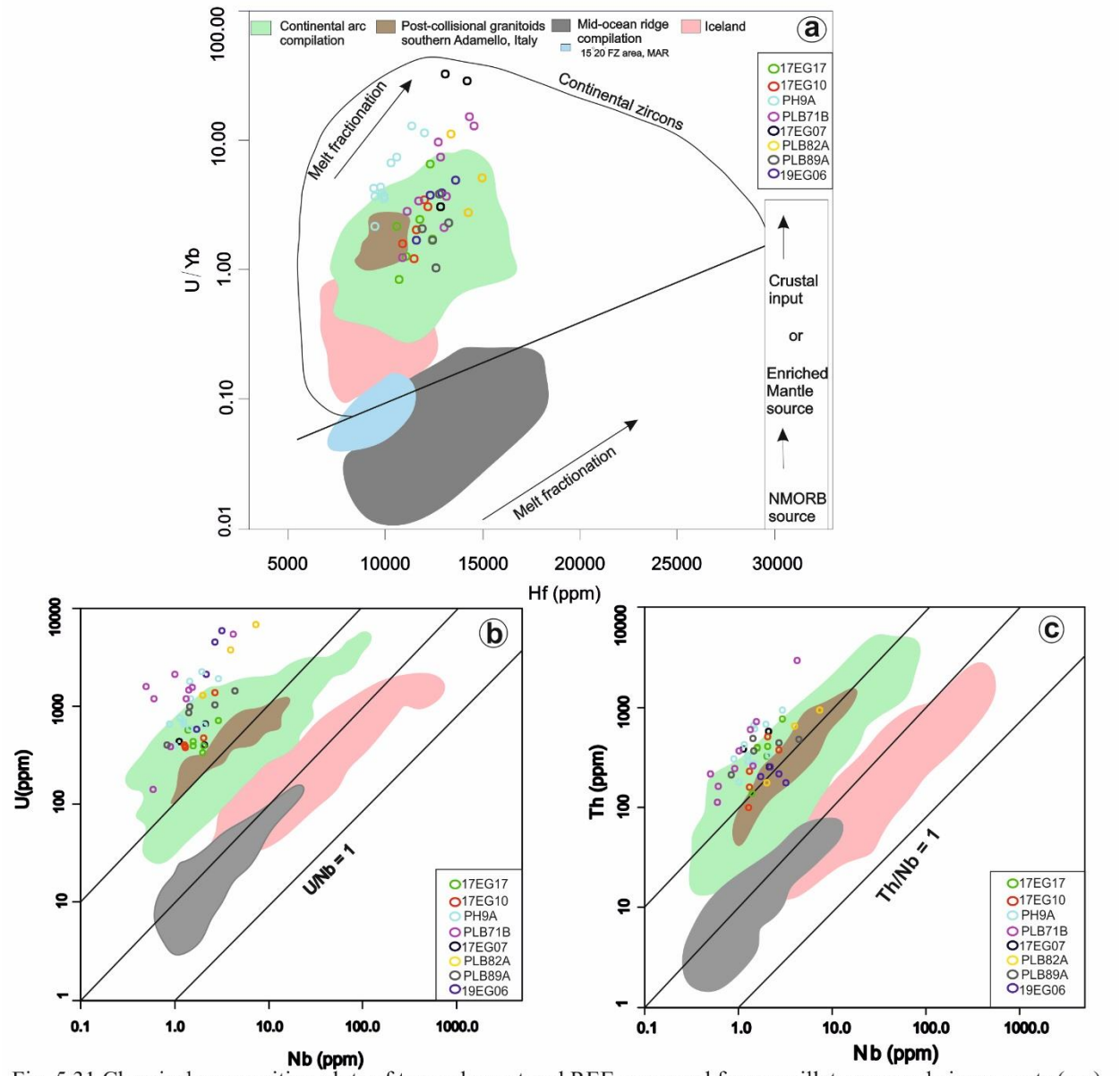

Fig. 5.31 Chemical composition plots of trace element and REE measured from oscillatory-zoned zircon spots (a-c). Circles having different colours represent different samples. Different composition fields shown in the diagram are after Grimes et al. (2007, 2015). (a) U/Yb vs Hf plot. (b) U vs Nb plot. (c) Th vs Nb plot.

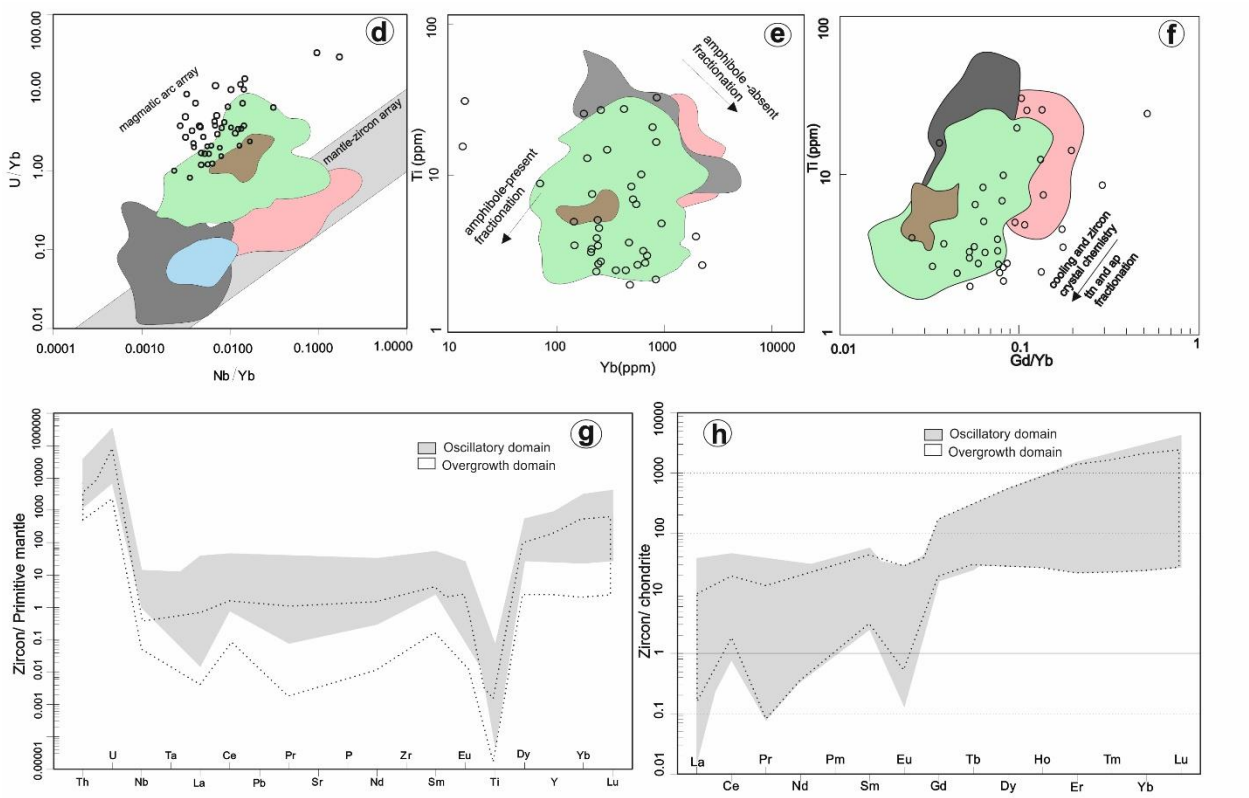

Fig. 5.31Chemical composition plots of trace element and REE measured from oscillatory-zoned zircon spots (d-h). (d) U/Yb vs Nb/Yb plot. (e) Ti vs Yb and (f) Ti vs Gd/Yb plot. (g) Multi-element trace and REE plot normalized to primitive mantle (Sun and McDonough, 1989). Colours used are same as used in (a-f). Note the prominent depletion of Ti and La and enrichment of U. Also note the flat to slightly enriched HREE plots. (h) Chondrite-normalized (after McDonough and Sun, 1995) REE pattern of the analyzed zircon showing prominent depletion in Pr and Eu and enrichment of Ce and Sm. Excepting a few samples (flat HREE pattern), most samples show enriched HREE pattern.

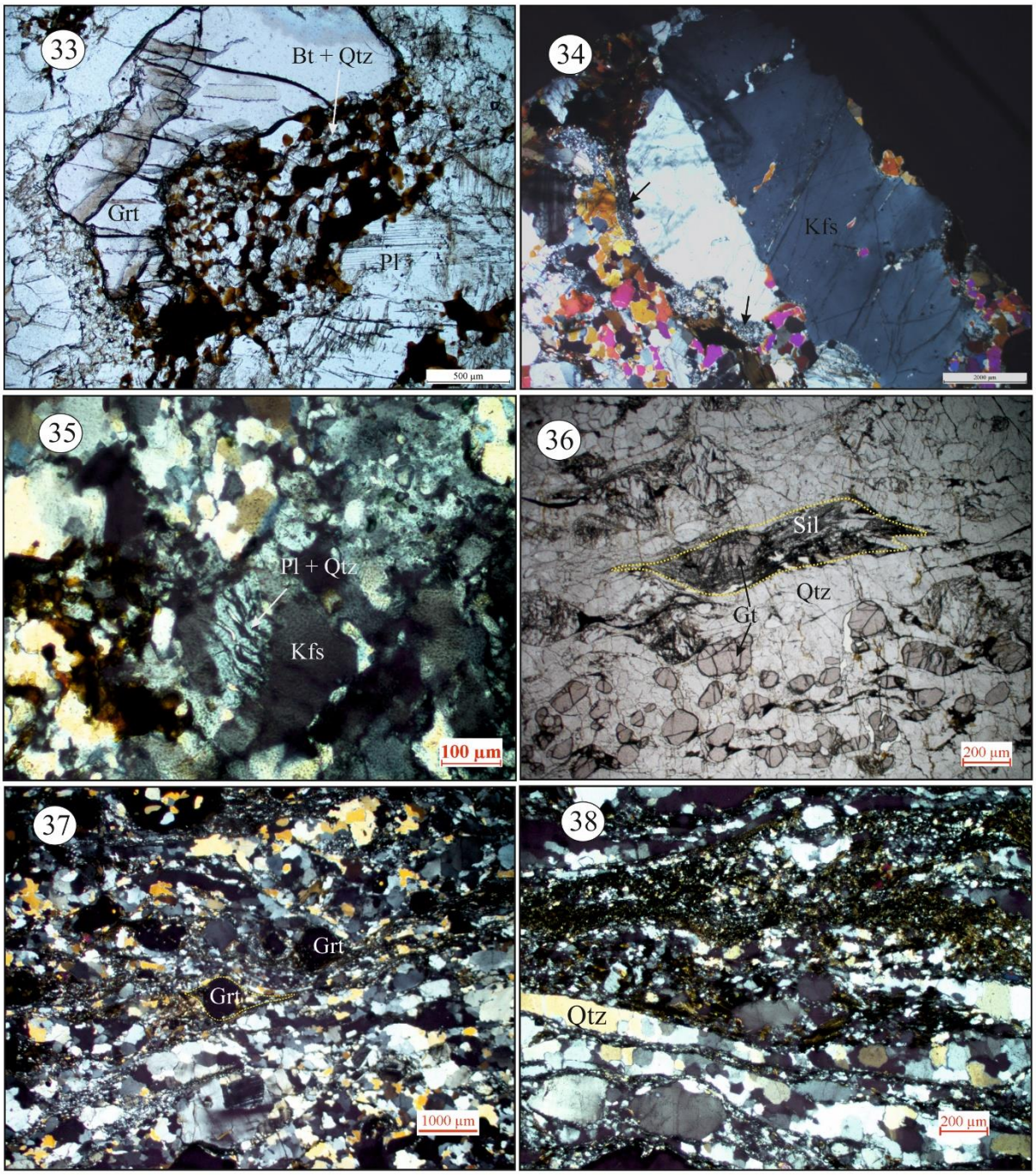

Fig. 5. Photomicrographs of granites. (33) Symplectic intergrowth of biotite (Bt) + quartz (Qtz) on porphyroblastic garnet (Grt). (34) Large k-feldspar (Kfs) grain show subgrain formation and recrystallization. (35) Cuspate grain boundary and intergrowth between plagioclase (Pl) and quartz (Qtz), forming myrmekitic texture. (36) Micro-enclaves of aluminous granulite within granite containing mineral assemblage like sillimanite (Sil) + spinel + haemo-ilmenite grains. (37) Symmetric-asymmetric tails around garnet (Grt) within mylonitized granite. (38) Fine recrystallized matrix grains and quartz (Qtz) ribbons in mylonitized granite.

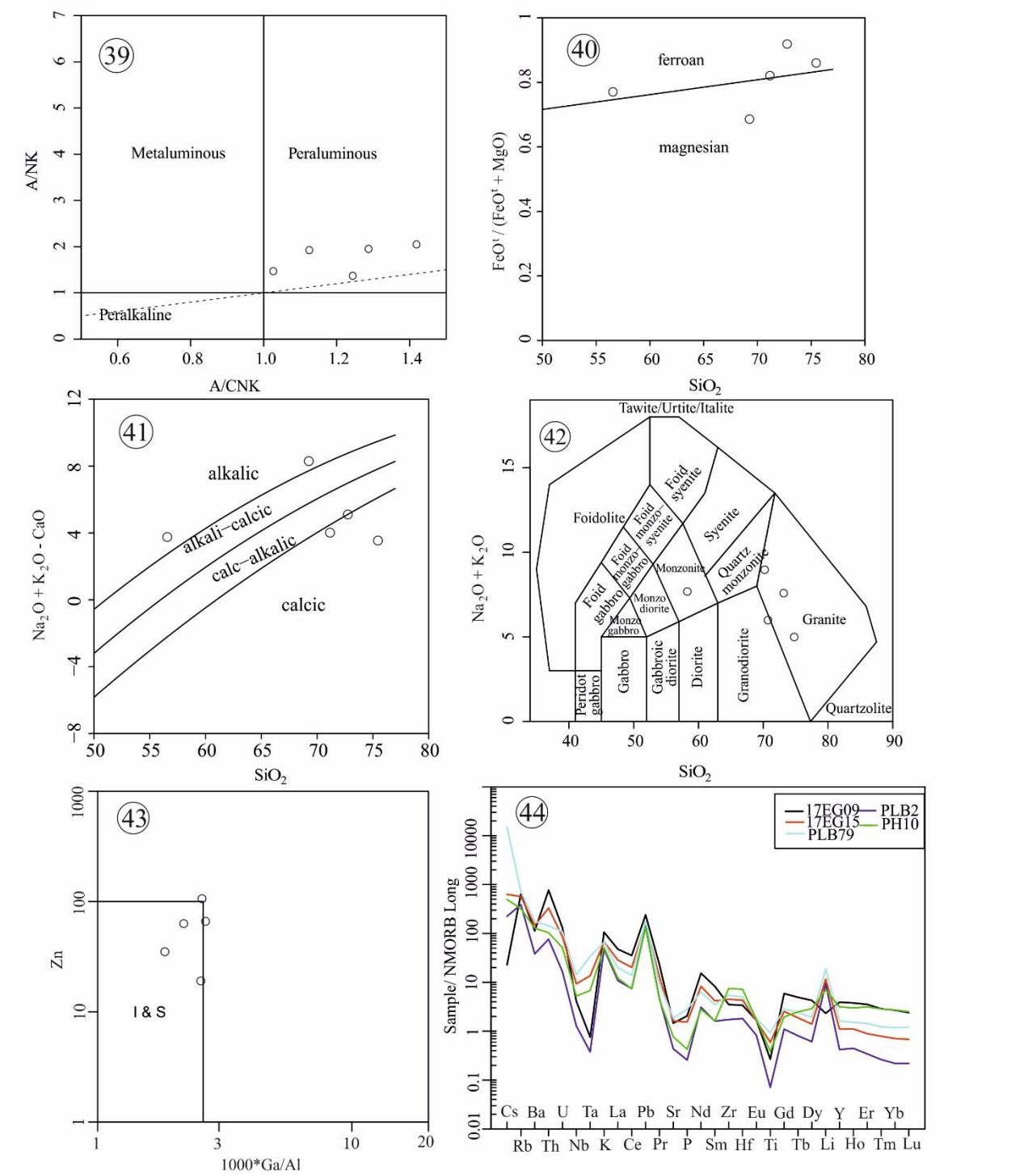

Fig. 5. Geochemical plots of granites. (39) ASI vs A/NK plot after Frost et al., (2001) show peraluminous character. (40) SiO_2 vs FeO_t plot after Frost et al., (2001) show ferroan character. (41) MALI plot after Frost et al., (2001) show broad range from calcic to alkali. (42) Total alkali vs silica (TAS) diagram plot after Middlemost (1994). (43) 1000*Ga/Al vs Zn plot after Whalen (1987). (44) Trace element plot after Sun and McDonough (1989), normalized to MORB values. Note that the plot show enriched Rb, Th, K, Pb and Li and depleted Ba, Nb, Ta, Sr, P and Ti.

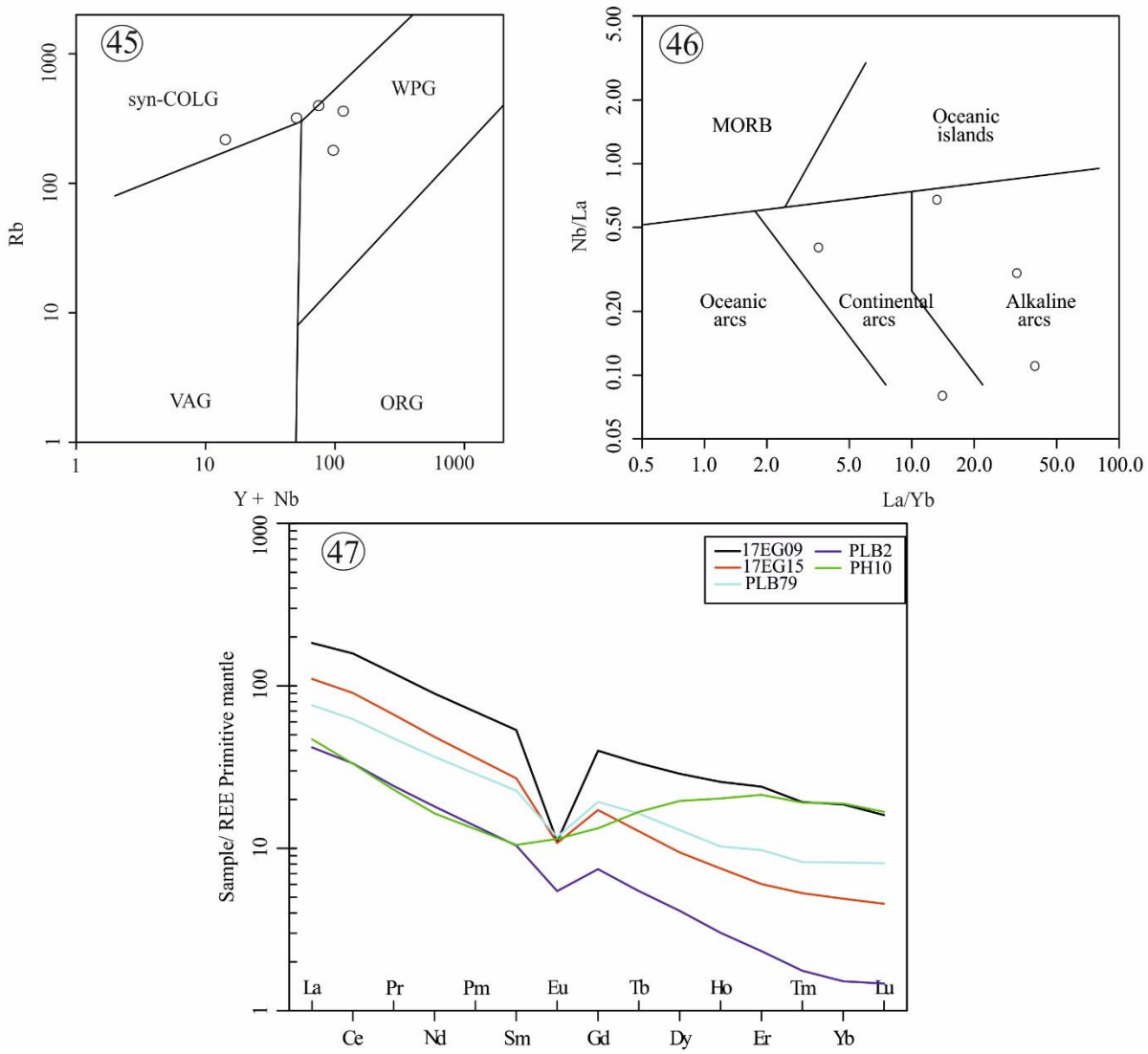

Fig. 5. (45) Rb vs Y + Nb plot after Pearce et al., (1984) show overlapping characteristicbetween syn-collisional and within plate granite. (46) Nb/La vs La/Yb plot after Hollocher (2012) show arc signature. (47) REE) normalized to the primitive mantle (McDonough and Sun, 1995) show enriched LREE and depleted HREE trend.

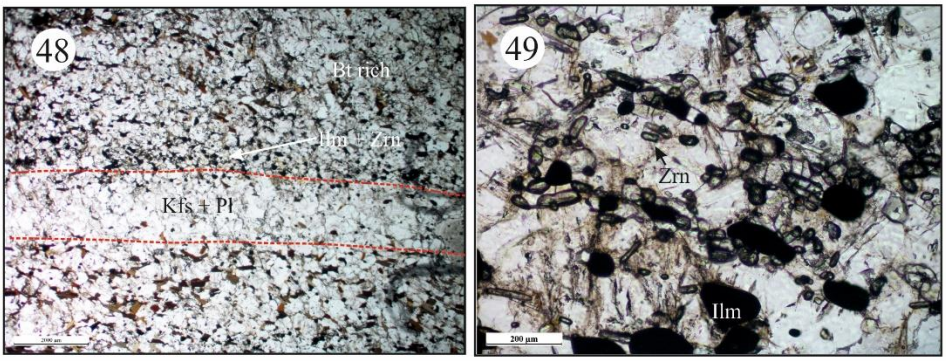

Fig.5. Photomicrographs of monzosyenite (48) Magmatic layering with alternate biotite-rich and plagioclase (Pl) + K-feldspar (Kfs)-rich layers. (49) Clusters of zircon (Zrn) occur in association with ilmenite (Ilm), biotite (Bt) and plagioclase (Pl) (both under PPL).

Table 5.1. GPS location, mineral association, important textures and calculated ages of different felsic granulites.

Sample no.	Rock	GPS location	Mineral association (mode%)	Structure	Important texture	Age calculated
17EG07	Charnockite	18°15'02"N 82°47'52.3"E	Qtz (23%), Pl (14%), Kfs (19%), Grt (21%), Opx (11%), Ilm (2%), Bt (<6%), Zrn +Ap+Py+Po+Cp (<5%)	Massive	Garanoblastic polygonal	**939±27** Ma (crystallization age) ca. 869–754 Ma (metamorphic age)
17EG10	Charnockite	18°3' 40.7"N 82°35'15"E	Qtz (21%), Pl (17%), Kfs (21%), Grt (23%), Opx (8%), Ilm(5%), Bt (5%), Zrn (~1%), Ap (<2%)	Foliated	Granoblastic and Grt_2+Qtz corona on Opx and Ilm	**1002±13** Ma (crystallization age) ca. 886–814 Ma (metamorphic age)
17EG12	Charnockite	18°10'15.1"N 82°44'08.6"E	Qtz (19%), Pl (25%),Kfs (17%), Grt (18%), Opx (<10%), Ilm (7%), Bt (<5%), Zrn + Ap (<3%)	Massive	Grt_2+Qtz corona on Opx	
17EG17	Charnockite	18°15'42.9"N 83°01'57.3"E	Qtz (25%), Kfs(21%), Pl(18%), Grt (21%),Opx (8%), Bt (5%)	Massive	Grt_2+Qtz corona on Opx	**951±9** Ma (crystallization age) ca. 931–819 Ma (metamorphic age)
17EG18B	Charnockite	18°13'33.4"N 82°00'29.1"E	Qtz (17%), Kfs (15%), Pl (22%), Opx (13%), Ilm (<5%), Bt (8%), Grt (18%), Ap (<3%), Zrn (<2%)	Foliated	Gneissic fabric: alternate Opx-Ilm and Qtz-Kfs-Pl layers	
S 26	Charnockite	18°16'13.0"N 82°57'7.3"E	Qtz (23%), Pl (14%), Kfs (17%), Grt (19%), Bt (<5%), Ilm (7%), Opx (8%), Ap (<5%), Zrn (<3%)	Massive	Grt_2+Qtz corona on Opx	
17EG13	Charnockite	18°17'09.5"N 82°57'7.3"E	Grt (25%), Qtz (23%), Pl (21%), Kfs (14%), Opx (9%), Bt (7%), Ilm (<2%)	Massive	Granoblastic polygonal	
PLB71B	Charnockite	20°40'30.2"N 84°23'16.8"E	Opx (19%), Pl (21%), Kfs (12%), Qtz (21%), Grt (7%), Bt (8%), Hem (5%), Py+Po (<3%), Zrn (<2%), Ap (2%)	Intrusive	Grt_2 +Qtz corona on Ilm	**951±13** Ma (crystallization age) ca. 931–896 Ma (metamorphic age)
PLB89A	Charnockite	20°35'3.5"N 84°31'38.9"E	Qtz (23%), Kfs (19%), Pl (23%), Cpx (11%), Grt (9%), Bt (7%), Hbl (<5%)	Foliated	Ilm + Kfs intergrowth on Bt	**978±16** Ma (crystallization age) ca. 915–859 Ma (metamorphic age)
PLB7/2	Charnockite	20°34'23.34"N 84°18'33.16"E	Qtz (20%), Pl (23%), Kfs (17%), Opx (<5%), Grt (15%), Bt (8%), Ilm (<5%), Hbl (3%).	Intrusive	Grt_2 corona separating Opx and Pl	
PLB2b	Charnockite	20°33'55.06"N 84°18'30.73"E	Opx (27%), Grt (9%), Pl (22%), Kfs (14%), Qtz (17%), Bt (<5%), Ap (<2%), Ilm (5%), Zrn (<1%)	Foliated	Grt_2 corona on Opx	
PH12	Charnockite	20°23'48.6"N 84°12'32.62"E	Opx (27%), Qtz (23%), Pl (14%), Kfs (18%), Bt (7%), Ilm (3%), Hbl (<5%), Ap (<3%)	Massive	Granoblastic polygonal	
PLB82A	Charnockite	20°17'15.6"N 84°18'5.7"E	Opx (8%), Qtz (33%), Kfs (23%), Pl (19%), Bt (10%), Ilm (3%), Ap (<2%), Zrn (<2%)	Massive	Bt+Qtz symplectite around Grt_1	**966±22** Ma (crystallization age) ca. 925–813 Ma (metamorphic age)
19EG06	Charnockite	18°17'41.13"N 83°53'27.96"E	Opx (11%), Qtz (23%),Pl (31%),Kfs (21%), Bt (8%), Ilm (3%), Zrn (<2%)	Massive	Granoblastic polygonal	**954±8** Ma (crystallization age) ca. 925–845 Ma (metamorphic age)
PH9A	Charnockite	20°27'30"N 84°12'48" E	Opx (14%), Qtz (21%), Pl (21%), Kfs (15%), Gt (11%), Bt (8%), Hbl (6%), Ilm (2%), Zrn (<2%)	Foliated	Intergrowth of Grt_2 + Qtz around Opx and Ilm.	**1020±16** Ma (crystallization age) ca. 949–927 Ma (metamorphic age)
PH48	Charnockite	20°20´29.66"N 84°17´8.03"E	Gt (8%), Opx (11%), Qtz (23%), Pl (21%), Kfs (19%), Ilm (7%), Bt (8%), Ap (2%), Zrn (<1%)	Massive	Grt_2 +Qtz corona on Opx	
17EG09	Granite	18°04' 0.1"N 82°37'51.1"E	Gt (11 %), Qtz (31%), Kfs (27%), Pl (17%), Bt (8%), Ilm (3%), Ap (<2%), Zrn (<2%)	Massive	Granoblastic polygonal	
17EG15	Granite	18°14' 57.9"N 82°59'42.3"E	Gt (13%), Qtz (33%), Kfs (23%), Pl (19%), Ilm (5%), Ap (<3%), Zrn (<2%)	Massive	Granoblastic polygonal	
PLB2	Granite	20°33'55.06"N 84°18'30.73"E	Pl(27%), Kfs (23%), Qtz (33%), Bt (5%), Ilm (7%), Zrn (<2%)	Massive	Granoblastic polygonal	
PLB79	Granite	19°59'47.90"N 83°42'4.70"E	Gt (15%), Bt (7%), Pl (23%), Kfs (19%), Qtz (27%), Ilm (7%), Ap (<3%)	Massive	Granoblastic polygonal	
PH10	Mylonitized Granite gneiss	20°24'33.85"N 84°12'38.47"E	Gt (13%), Bt (11%), Qtz (29%), Pl (17%), Kfs (19%), Sill (7%), Ap (3%)	Foliated	Mylonitized	
BLG3C	Monzosyenite	20°39'59.69"N 83°10'39.08"E	Pl (35 %), Qtz (17%), Kfs (31%), Bt (11%), Zrn (4%), Ilm (3%)	Dyke		**490 ± 3** Ma (crystallization age)

Table 5.2. Representative mineral chemical data from charnockite samples.

Sample	17EG18B												PLB2B			
Phase	Grt_1	Grt_1	Grt_1	Grt_1	Grt_1	Grt_1	Grt_1	Grt_2	Grt_2	Grt_2	Grt_2	Grt_2	Grt_2	Grt_2	Grt_2	Grt_2
Anal. no.	1	2	6	15	16	44	45	12	27	28	52	61	31	32	36	39
SiO_2	38.38	38.39	38.59	38.64	38.44	38.85	38.81	38.23	38.75	37.98	39.38	38.94	37.41	37.48	37.41	37.46
TiO_2	0.05	0.04	0.05	0.30	0.17	0.04	0.04	0.06	0.03		0.13	0.02	0.01	0.01		0.05
Al_2O_3	20.79	20.87	21.13	21.04	21.06	21.1	21.16	20.8	21.1	20.81	21.63	21.32	20.41	20.32	19.97	20.42
Cr_2O_3	0.02	0.02	0.01	0.04	0.01	0.02	0.03	0.02	0.01	0.02	0.02	0.02	0.03		0.01	0.04
Fe_2O_3	1.27	1.55	0.99	0.00	0.23	0.38	0.56	0.00	0.00	0.85	0.00	0.00	2.15	2.38	1.60	1.90
FeO	27.82	26.72	27.29	30.26	29.55	28.12	27.92	31.05	33.24	30.43	31.74	29.09	29.65	29.16	29.62	30.17
MnO	0.73	0.72	0.73	0.74	0.73	0.75	0.75	0.82	0.75	0.76	0.73	0.77	1.24	1.15	1.28	1.29
MgO	7.84	8.28	8.12	6.84	7.07	7.97	7.94	6.13	5.39	6.47	6.56	7.83	3.38	3.40	3.30	3.25
CaO	2.66	2.91	2.88	2.55	2.52	2.66	2.82	2.31	2.15	2.09	2.37	2.15	6.10	6.59	6.19	5.91
Total	99.56	99.51	99.79	100.41	99.77	99.89	100.03	99.42	101.42	99.42	102.56	100.14	100.38	100.49	99.38	100.49
O-basis	12	12	12	12	12	12	12	12	12	12	12	12	12	12	12	12
Si	3.001	2.993	3.000	3.022	3.011	3.019	3.013	3.029	3.053	3.004	3.054	3.030	2.977	2.977	3.006	2.981
Ti	0.003	0.002	0.003	0.018	0.010	0.002	0.002	0.004	0.002		0.008	0.001	0.001	0.001		0.003
Al	1.916	1.917	1.936	1.939	1.944	1.933	1.936	1.943	1.960	1.940	1.977	1.955	1.914	1.902	1.891	1.915
Cr	0.001	0.001	0.001	0.002	0.001	0.001	0.002	0.001	0.001	0.001	0.001	0.001	0.002		0.001	0.003
Fe^{3+}	0.075	0.091	0.058		0.013	0.022	0.033			0.051			0.129	0.142	0.097	0.114
Fe^{2+}	1.819	1.742	1.774	1.979	1.935	1.828	1.812	2.058	2.190	2.013	2.059	1.893	1.973	1.937	1.991	2.008
Mn	0.048	0.048	0.048	0.049	0.048	0.049	0.049	0.055	0.050	0.051	0.048	0.051	0.084	0.077	0.087	0.087
Mg	0.914	0.962	0.941	0.797	0.826	0.923	0.919	0.724	0.633	0.763	0.758	0.908	0.401	0.403	0.395	0.386
Ca	0.223	0.243	0.240	0.214	0.211	0.222	0.235	0.196	0.182	0.177	0.197	0.179	0.520	0.561	0.533	0.504
Cation	8	8	8	8	8	8	8	8	8	8	8	8	8	8	8	8
X_{Mg}	0.33	0.36	0.35	0.29	0.30	0.34	0.34	0.26	0.22	0.27	0.27	0.32	0.17	0.17	0.17	0.16
X_{Alm}	0.61	0.58	0.59	0.65	0.64	0.60	0.60	0.68	0.72	0.67	0.67	0.62	0.66	0.65	0.66	0.67
X_{Prp}	0.30	0.32	0.31	0.26	0.27	0.31	0.30	0.24	0.21	0.25	0.25	0.30	0.13	0.14	0.13	0.13
X_{Grs}	0.07	0.08	0.08	0.07	0.07	0.07	0.08	0.06	0.06	0.06	0.07	0.06	0.16	0.18	0.17	0.16
X_{Sps}	0.02	0.02	0.02	0.02	0.02	0.02	0.02	0.02	0.02	0.02	0.02	0.02	0.03	0.03	0.03	0.03
X_{and}	0.00	0.00	0.00	0.00	0.00	0.00	0.00	0.00	0.00	0.00	0.00	0.00	0.01	0.01	0.01	0.01

Table 5.2. Continued.

Sample	PLB2B										S26					
Phase	Grt_2	Grt_2	Grt_2	Grt_2	Grt_2	Grt_2	Grt_2	Grt_2	Grt_2	Grt_2	Grt_1	Grt_1	Grt_1	Grt_1	Grt_1	Grt_1
Anal. no.	40	41	42	43	50	52	56	57	68	69	1	2	3	50	51	62
SiO_2	37.67	37.27	37.30	37.41	37.45	37.50	37.51	37.74	37.65	37.60	37.60	37.94	37.68	37.59	37.79	38.39
TiO_2		0.06	0.03	0.02	0.02	0.05	0.02	0.04	0.04	0.05	0.06	0.05	0.09	0.03	0.04	0.05
Al_2O_3	20.39	20.32	20.33	20.35	20.28	20.45	20.49	20.42	20.53	20.35	20.47	20.54	20.59	20.59	20.60	20.76
Cr_2O_3		0.03	0.04	0.05	0.01		0.04	0.06	0.00	0.03	0.03	0.02	0.04	0.03	0.03	0.03
Fe_2O_3	1.36	2.22	2.20	1.93	2.17	1.55	1.57	1.78	1.64	1.13	1.63	1.19	1.59	0.46	1.60	0.00
FeO	30.33	29.65	29.90	29.68	29.87	29.80	30.12	30.09	29.38	29.90	28.48	28.41	28.41	30.43	28.88	29.89
MnO	1.20	1.21	1.27	1.25	1.19	1.06	1.09	1.10	1.09	1.12	0.86	0.89	0.84	0.91	0.80	0.82
MgO	3.24	3.40	3.19	3.49	3.35	3.47	3.42	3.47	3.45	3.34	5.84	6.05	5.90	4.79	5.93	5.79
CaO	6.03	6.00	6.05	5.92	6.05	6.11	5.89	6.07	6.57	6.26	4.10	4.15	4.18	3.97	3.87	3.83
Total	100.22	100.15	100.31	100.10	100.39	99.98	100.16	100.77	100.35	99.77	99.07	99.24	99.32	98.80	99.54	99.56
O-basis	12	12	12	12	12	12	12	12	12	12	12	12	12	12	12	12
Si	3.002	2.974	2.975	2.983	2.982	2.990	2.988	2.989	2.988	3.004	2.988	3.003	2.985	3.011	2.989	3.032
Ti		0.004	0.002	0.001	0.001	0.003	0.001	0.002	0.002	0.003	0.004	0.003	0.005	0.002	0.002	0.003
Al	1.915	1.911	1.911	1.912	1.903	1.922	1.924	1.906	1.921	1.916	1.917	1.916	1.922	1.944	1.920	1.932
Cr		0.002	0.003	0.003	0.001		0.003	0.004		0.002	0.002	0.001	0.003	0.002	0.002	0.002
Fe^{3+}	0.081	0.133	0.132	0.116	0.130	0.093	0.094	0.106	0.098	0.068	0.098	0.071	0.094	0.028	0.095	0.000
Fe^{2+}	2.021	1.978	1.995	1.979	1.989	1.987	2.007	1.993	1.951	1.998	1.893	1.880	1.882	2.039	1.911	1.974
Mn	0.081	0.082	0.086	0.084	0.080	0.072	0.074	0.074	0.073	0.076	0.058	0.060	0.056	0.062	0.054	0.055
Mg	0.385	0.404	0.379	0.415	0.398	0.412	0.406	0.410	0.408	0.398	0.692	0.714	0.697	0.572	0.699	0.682
Ca	0.515	0.513	0.517	0.506	0.516	0.522	0.503	0.515	0.559	0.536	0.349	0.352	0.355	0.341	0.328	0.324
Cation	8	8	8	8	8	8	8	8	8	8	8	8	8	8	8	8
X_{Mg}	0.16	0.17	0.16	0.17	0.17	0.17	0.17	0.17	0.17	0.17	0.27	0.28	0.27	0.22	0.27	0.26
X_{Alm}	0.67	0.66	0.67	0.66	0.67	0.66	0.67	0.67	0.65	0.66	0.63	0.63	0.63	0.68	0.64	0.65
X_{Prp}	0.13	0.14	0.13	0.14	0.13	0.14	0.14	0.14	0.14	0.13	0.23	0.24	0.23	0.19	0.23	0.22
X_{Grs}	0.16	0.16	0.16	0.16	0.16	0.17	0.16	0.16	0.18	0.17	0.11	0.11	0.11	0.11	0.10	0.11
X_{Sps}	0.03	0.03	0.03	0.03	0.03	0.02	0.02	0.02	0.02	0.03	0.02	0.02	0.02	0.02	0.02	0.02
X_{and}	0.01	0.01	0.01	0.01	0.01	0.01	0.01	0.01	0.01	0.01	0.01	0.00	0.01	0.00	0.01	0.00

Table 5.2. Continued.

Sample	S26								17EG07							
Phase	Grt_1	Grt_1	Grt_2	Grt_2	Grt_2	Grt_2	Grt_2	Grt_2	Grt_1	Grt_1	Grt_1	Grt_1	Grt_1	Grt_1	Grt_1	Grt_1
Anal. no.	72	93	6	17	28	29	66	70	52	53	58	62	69	72	73	76
SiO_2	38.01	37.55	37.81	37.56	37.78	37.36	37.51	37.96	38.48	37.94	37.79	38.20	38.03	38.11	38.14	38.03
TiO_2	0.03	0.04	0.03	0.05	0.02	0.06	0.05	0.04	0.04	0.02	0.01	0.02	0.00	0.04	0.03	0.00
Al_2O_3	20.75	20.42	20.59	20.51	20.65	20.52	20.63	20.64	21.11	20.82	20.95	21.05	20.79	20.87	21.07	20.89
Cr_2O_3	0.06	0.04	0.02	0.02	0.03		0.02	0.03	0.03	0.06	0.05	0.00	0.06	0.05	0.06	0.03
Fe_2O_3	0.38	1.26	1.42	1.12	0.69	2.05	1.32	1.17	0.00	0.20	0.48	0.00	0.33	0.11	0.00	0.54
FeO	29.41	30.12	28.9904	28.63	28.52	27.65	29.25	29.21	31.17	30.53	30.17	29.86	30.61	30.19	30.64	29.13
MnO	0.79	0.92	0.83	0.84	0.81	0.81	0.84	0.83	0.73	0.73	0.68	0.71	0.69	0.72	0.74	0.71
MgO	5.95	4.98	5.79	5.7	5.96	6.25	5.64	5.72	4.26	4.93	4.78	4.91	4.93	4.69	5.07	4.89
CaO	3.64	3.91	3.97	4.15	4.08	3.99	3.7	4.04	5.11	4.16	4.54	4.97	4.20	4.94	4.06	5.39
Total	99.02	99.24	99.45	98.58	98.54	98.70	98.96	99.65	100.93	99.39	99.45	99.72	99.63	99.72	99.81	99.61
O-basis	12	12	12	12	12	12	12	12	12	12	12	12	12	12	12	12
Si	3.015	2.998	2.994	2.998	3.008	2.973	2.988	3.000	3.036	3.016	3.003	3.022	3.017	3.019	3.019	3.009
Ti	0.002	0.002	0.002	0.003	0.001	0.004	0.003	0.002	0.002	0.001	0.001	0.001	0.000	0.002	0.002	
Al	1.940	1.921	1.922	1.929	1.938	1.924	1.937	1.923	1.963	1.950	1.962	1.962	1.944	1.948	1.965	1.948
Cr	0.004	0.003	0.001	0.001	0.002	0.000	0.001	0.002	0.002	0.004	0.003	-0.001	0.004	0.003	0.004	0.002
Fe^{3+}	0.023	0.076	0.085	0.067	0.041	0.123	0.079	0.070	0.000	0.012	0.029	0.000	0.019	0.007	0.000	0.032
Fe^{2+}	1.951	2.011	1.920	1.911	1.899	1.840	1.949	1.931	2.057	2.029	2.005	1.975	2.030	2.000	2.028	1.928
Mn	0.053	0.062	0.056	0.057	0.055	0.055	0.057	0.056	0.049	0.049	0.046	0.048	0.046	0.048	0.050	0.048
Mg	0.704	0.593	0.684	0.678	0.707	0.741	0.670	0.674	0.501	0.584	0.566	0.579	0.583	0.554	0.598	0.577
Ca	0.309	0.334	0.337	0.355	0.348	0.340	0.316	0.342	0.432	0.354	0.387	0.421	0.357	0.419	0.344	0.457
Cation	8	8	8	8	8	8	8	8	8	8	8	8	8	8	8	8
X_{Mg}	0.27	0.23	0.26	0.26	0.27	0.29	0.26	0.26	0.20	0.22	0.22	0.23	0.22	0.22	0.23	0.23
X_{Alm}	0.65	0.67	0.64	0.64	0.63	0.62	0.65	0.64	0.68	0.67	0.67	0.65	0.67	0.66	0.67	0.64
X_{Prp}	0.23	0.20	0.23	0.23	0.24	0.25	0.22	0.22	0.16	0.19	0.19	0.19	0.19	0.18	0.20	0.19
X_{Grs}	0.10	0.11	0.11	0.11	0.11	0.11	0.10	0.11	0.15	0.12	0.13	0.14	0.12	0.14	0.11	0.15
X_{Sps}	0.02	0.02	0.02	0.02	0.02	0.02	0.02	0.02	0.02	0.02	0.02	0.02	0.02	0.02	0.02	0.02
X_{and}	0.00	0.00	0.00	0.00	0.00	0.01	0.00	0.00	0.00	0.00	0.00	0.00	0.00	0.00	0.00	0.00

Table 5.2. Continued.

Sample	17EG07											PLB7/2				
Phase	Grt_1	Grt_1	Grt_2	Grt_2	Grt_2	Grt_2	Grt_2	Grt_2	Grt_2	Grt_2	Grt_2	Grt_1	Grt_1	Grt_1	Grt_1	Grt_1
Anal. no.	79	89	3	4	6	8	9	10	11	86	87	3	4	5	6	9
SiO_2	37.93	38.06	38.23	37.82	39.28	37.83	37.46	37.08	37.36	37.95	37.94	37.03	37.06	37.02	37.14	36.96
TiO_2	0.02	0.05	0.49	0.04	0.01	0.05	0.29	0.43	0.13	0.05	0.02	0.10	0.04	0.01	0.01	0.04
Al_2O_3	20.89	20.99	20.17	20.55	21.38	20.49	20.39	20.40	20.40	20.95	20.95	20.13	20.2	20.41	20.22	20.02
Cr_2O_3	0.05	0.02	0.05	0.05	0.04	0.08	0.04	0.05	0.02	0.08	0.04	0.05	0.03	0.02		0.02
Fe_2O_3	0.45	0.00	0.00	0.03	0.00	0.46	0.00	0.32	0.53	0.20	0.63	0.60	0.99	1.39	1.35	1.42
FeO	30.35	30.96	31.74	30.07	34.20	29.32	30.73	30.65	30.00	30.97	29.30	31.58	33.94	30.86	29.86	29.42
MnO	0.71	0.68	0.87	0.77	0.88	0.72	0.89	0.94	0.85	0.71	0.62	0.87	1.03	0.94	0.88	0.82
MgO	5.10	3.90	4.47	4.16	2.76	4.63	3.65	3.46	3.84	3.86	4.76	2.8	3.36	2.71	2.35	2.43
CaO	4.07	5.43	4.34	5.46	5.44	5.45	5.40	5.43	5.53	5.35	5.44	5.4	2.64	5.96	7.4	7.53
Total	99.56	100.09	100.36	98.95	103.99	99.03	98.85	98.76	98.66	100.12	99.70	98.56	99.29	99.32	99.20	98.66
O-basis	12	12	12	12	12	12	12	12	12	12	12	12	12	12	12	12
Si	3.008	3.021	3.060	3.026	3.092	3.018	3.018	2.992	3.008	3.010	3.002	3.010	3.002	2.986	2.997	2.997
Ti	0.001	0.003	0.029	0.002	0.001	0.003	0.018	0.026	0.008	0.003	0.001	0.006	0.002	0.001	0.001	0.002
Al	1.952	1.964	1.903	1.938	1.983	1.926	1.936	1.940	1.936	1.958	1.954	1.928	1.929	1.940	1.923	1.913
Cr	0.003	0.001	0.003	0.003	0.002	0.005	0.003	0.003	0.001	0.005	0.003	0.003	0.002	0.001	0.000	0.001
Fe^{3+}	0.027			0.002		0.028	0.000	0.020	0.032	0.012	0.038	0.037	0.061	0.085	0.082	0.087
Fe^{2+}	2.013	2.055	2.125	2.012	2.251	1.956	2.070	2.068	2.020	2.054	1.939	2.146	2.299	2.082	2.015	1.995
Mn	0.048	0.046	0.059	0.052	0.059	0.049	0.061	0.064	0.058	0.048	0.042	0.060	0.071	0.064	0.060	0.056
Mg	0.603	0.462	0.533	0.496	0.324	0.551	0.438	0.416	0.461	0.456	0.561	0.339	0.406	0.326	0.283	0.294
Ca	0.346	0.462	0.372	0.468	0.459	0.466	0.466	0.470	0.477	0.455	0.461	0.470	0.229	0.515	0.640	0.654
Cation	8	8	8	8	8	8	8	8	8	8	8	8	8	8	8	8
X_{Mg}	0.23	0.18	0.20	0.20	0.13	0.22	0.17	0.17	0.19	0.18	0.22	0.14	0.15	0.14	0.12	0.13
X_{Alm}	0.67	0.68	0.69	0.66	0.73	0.65	0.68	0.69	0.67	0.68	0.65	0.71	0.77	0.70	0.67	0.67
X_{Prp}	0.20	0.15	0.17	0.16	0.10	0.18	0.14	0.14	0.15	0.15	0.19	0.11	0.14	0.11	0.09	0.10
X_{Grs}	0.11	0.15	0.13	0.15	0.16	0.15	0.15	0.15	0.16	0.15	0.15	0.15	0.07	0.17	0.20	0.21
X_{Sps}	0.02	0.02	0.02	0.02	0.02	0.02	0.02	0.02	0.02	0.02	0.01	0.02	0.02	0.02	0.02	0.02
X_{and}	0.00	0.00	0.00	0.00	0.00	0.00	0.00	0.00	0.00	0.00	0.00	0.00	0.00	0.01	0.01	0.01

Table 5.2. Continued.

Sample	PLB7/2						PLB89A								
Phase	Grt_2	Grt_2	Grt_2	Grt_2	Grt_2	Grt_2	Grt_1	Grt_1	Grt_1	Grt_1	Grt_1	Grt_1	Grt_2	Grt_2	Grt_2
Anal. no.	16	17	20	21	25	28	3	4	5	6	44	45	10	14	36
SiO_2	37.19	37.05	37.54	37.39	37.2	37.27	37.51	37.44	37.67	37.49	37.51	37.86	37.62	37.92	37.36
TiO_2	0.02	0.01	0.03	0.05	0.30	0.06	0.06		0.01	0.02	0.05		0.01	0.06	0.03
Al_2O_3	20.17	20.15	20.28	19.9	19.96	20.24	20.12	20.18	20.22	20.36	20.45	20.37	20.33	20.21	20.12
Cr_2O_3	0.05	0.02	0.01		0.03	0.02	0.03	0.01	0.01	0.04	0.01	0.03		0.03	
Fe_2O_3	0.68	1.38	0.65	0.89	1.16	0.88	1.05	1.08	1.15	1.38	0.68	0.83	0.54	0.15	1.37
FeO	29.45	29.62	30.06	30.29	29.57	29.87	29.91	29.41	29.53	29.41	29.84	30.03	29.94	31.23	29.52
MnO	0.82	0.89	0.86	0.82	0.83	0.71	1.16	1.19	1.19	1.15	1.16	1.11	1.27	1.21	1.15
MgO	2.35	2.44	2.21	2.36	2.29	2.3	2.63	2.57	2.59	2.69	2.75	2.74	2.22	2.07	2.56
CaO	7.82	7.37	7.84	7.36	8.01	7.75	7.13	7.47	7.57	7.4	7.01	7.21	7.66	7.22	7.38
Total	98.55	98.93	99.49	99.06	99.35	99.10	99.59	99.35	99.95	99.94	99.46	100.17	99.58	100.11	99.49
O-basis	12	12	12	12	12	12	12	12	12	12	12	12	12	12	12
Si	3.013	2.996	3.017	3.022	2.998	3.007	3.012	3.011	3.012	2.997	3.009	3.018	3.021	3.037	3.004
Ti	0.001	0.001	0.002	0.003	0.018	0.004	0.004		0.001	0.001	0.003		0.001	0.004	0.002
Al	1.926	1.921	1.921	1.896	1.896	1.925	1.904	1.913	1.905	1.918	1.934	1.913	1.924	1.908	1.906
Cr	0.003	0.001	0.001		0.002	0.001	0.002	0.001	0.001	0.003	0.001	0.002		0.002	
Fe^{3+}	0.041	0.084	0.040	0.054	0.070	0.053	0.063	0.065	0.069	0.083	0.041	0.050	0.033	0.009	0.083
Fe^{2+}	1.996	2.003	2.021	2.047	1.993	2.015	2.008	1.978	1.975	1.966	2.002	2.001	2.010	2.092	1.985
Mn	0.056	0.061	0.059	0.056	0.057	0.049	0.079	0.081	0.081	0.078	0.079	0.075	0.086	0.082	0.078
Mg	0.284	0.294	0.265	0.284	0.275	0.277	0.315	0.308	0.309	0.321	0.329	0.326	0.266	0.247	0.307
Ca	0.679	0.639	0.675	0.637	0.692	0.670	0.613	0.644	0.648	0.634	0.603	0.616	0.659	0.620	0.636
Cation	8	8	8	8	8	8	8	8	8	8	8	8	8	8	8
X_{Mg}	0.12	0.13	0.12	0.12	0.12	0.12	0.14	0.13	0.14	0.14	0.14	0.14	0.12	0.11	0.13
X_{Alm}	0.66	0.67	0.67	0.68	0.66	0.67	0.67	0.66	0.66	0.66	0.66	0.66	0.67	0.69	0.66
X_{Prp}	0.09	0.10	0.09	0.09	0.09	0.09	0.10	0.10	0.10	0.11	0.11	0.11	0.09	0.08	0.10
X_{Grs}	0.22	0.20	0.22	0.20	0.22	0.22	0.20	0.21	0.21	0.20	0.20	0.20	0.21	0.20	0.20
X_{Sps}	0.02	0.02	0.02	0.02	0.02	0.02	0.03	0.03	0.03	0.03	0.03	0.02	0.03	0.03	0.03
X_{and}	0.00	0.01	0.00	0.01	0.01	0.01	0.01	0.01	0.01	0.01	0.00	0.01	0.00	0.00	0.01

Table 5.2. Continued.

Sample	17EG18B															PLB2B					
Phase	Bt	Bt	Bt	Bt	Bt	Bt	Bt	Bt	Bt	Bt	Bt	Bt	Bt	Bt	Bt	Bt	Bt	Bt	Bt	Bt	Bt
Anal. no.	3	4	19	23	24	26	32	35	36	38	43	46	47	54	55	5	6	11	29	34	35
SiO_2	39.31	39.38	41.37	39.05	39.25	39.04	38.57	38.53	39.66	38.85	39.35	39.27	39.26	39.92	39.98	36.16	36.18	36.67	37.02	36.94	36.96
TiO_2	4.87	4.85	3.99	4.95	4.49	3.08	4.96	4.94	4.96	4.54	4.84	4.39	4.92	3.92	3.38	5.34	5.39	5.51	4.47	4.14	3.98
Al_2O_3	12.78	12.89	13.72	12.82	12.92	12.18	12.86	12.99	13.06	12.96	12.90	12.88	12.95	12.95	13.10	12.58	12.68	12.63	12.34	12.85	12.85
Cr_2O_3	0.01	0.04	0.03	0.03	0.01	0.03	0.02	0.05		0.04	0.02	0.04	0.04	0.03	0.03	0.04	0.05	0.06	0.02	0.04	0.02
FeO	7.86	8.34	7.14	8.69	9.03	11.04	9.97	9.88	10.73	9.95	10.68	7.85	7.67	5.72	5.76	19.52	19.49	19.20	18.48	16.72	17.27
MnO	0.01			0.02	0.04	0.02	0.01		0.02	0.01			0.01		0.01	0.07	0.04	0.04	0.05	0.01	0.02
MgO	18.97	18.90	19.21	18.11	17.92	17.98	17.21	17.21	16.58	17.56	16.60	19.15	18.53	21.04	21.85	11.55	11.81	11.76	12.76	14.14	13.85
CaO																					
ZnO	0.02	0.03	0.05	0.03		0.04	0.00	0.06	0.08		0.04	0.02	0.01	0.03			0.06	0.03	0.08	0.08	0.06
Na_2O	0.12	0.10	0.12	0.07	0.10	0.14	0.12	0.07	0.09	0.10	0.06	0.10	0.12	0.13	0.14	0.07	0.09	0.04	0.07	0.13	0.12
K_2O	9.09	9.41	9.17	9.20	9.21	9.08	9.25	9.22	8.95	9.14	8.66	9.28	9.01	9.30	9.25	8.34	8.51	8.90	8.10	8.59	8.49
P_2O_5		0.04	0.01		0.01	0.06			0.01		0.05	0.04	0.02			0.03	0.05	0.03	0.01		0.02
F	2.34	2.20	4.60	3.16	3.38	3.17	3.17	3.05	2.84	3.04	3.45	3.60	3.11	3.37	2.86	1.63	1.73	1.85	1.74	2.23	2.02
H_2O	2.96	3.05	2.01	2.55	2.44	2.48	2.51	2.57	2.73	2.59	2.40	2.36	2.58	2.52	2.78	3.09	3.06	3.03	3.06	2.86	2.95
Total	98.34	99.23	101.42	98.68	98.80	98.34	98.65	98.57	99.71	98.78	99.05	98.98	98.23	98.93	99.14	98.42	99.14	99.75	98.20	98.73	98.61
O-basis	11	11	11	11	11	11	11	11	11	11	11	11	11	11	11						
Si	5.791	5.769	5.924	5.786	5.820	5.871	5.758	5.750	5.839	5.778	5.845	5.794	5.805	5.820	5.799	5.617	5.588	5.626	5.719	5.659	5.673
Ti	0.540	0.534	0.430	0.552	0.501	0.348	0.557	0.554	0.549	0.508	0.541	0.487	0.547	0.430	0.369	0.624	0.626	0.636	0.519	0.477	0.459
Al	2.219	2.226	2.316	2.239	2.258	2.159	2.263	2.285	2.266	2.272	2.259	2.240	2.257	2.225	2.240	2.303	2.308	2.284	2.247	2.320	2.325
Cr	0.001	0.005	0.003	0.004	0.001	0.004	0.002	0.006	0.000	0.005	0.002	0.005	0.005	0.003	0.003	0.005	0.006	0.007	0.002	0.005	0.002
Fe^{2+}	0.968	1.022	0.855	1.077	1.120	1.389	1.245	1.233	1.321	1.238	1.327	0.969	0.948	0.697	0.699	2.536	2.517	2.464	2.387	2.142	2.217
Mn	0.001	0.000	0.000	0.003	0.005	0.003	0.001	0.000	0.002	0.001			0.001	0.000	0.001	0.009	0.005	0.005	0.007	0.001	0.003
Mg	4.166	4.128	4.100	4.000	3.961	4.031	3.830	3.828	3.639	3.893	3.676	4.212	4.084	4.573	4.724	2.674	2.719	2.690	2.938	3.229	3.169
Ca																					
Zn	0.002	0.003	0.005	0.003		0.004	0.000	0.007	0.009	0.000	0.004	0.004	0.004	0.003			0.007	0.003	0.009	0.009	0.007
Na	0.034	0.028	0.033	0.020	0.029	0.041	0.035	0.020	0.026	0.029	0.017	0.029	0.034	0.037	0.039	0.021	0.027	0.012	0.021	0.039	0.036
K	1.708	1.758	1.675	1.739	1.742	1.742	1.761	1.755	1.681	1.734	1.641	1.746	1.699	1.729	1.711	1.652	1.676	1.742	1.596	1.679	1.662
Cation	15.431	15.474	15.341	15.421	15.435	15.591	15.451	15.438	15.332	15.457	15.312	15.485	15.384	15.519	15.586	15.442	15.481	15.469	15.446	15.560	15.553
OH*	2.91	2.98	1.92	2.52	2.42	2.49	2.50	2.56	2.68	2.57	2.38	2.32	2.55	2.45	2.69	3.20	3.15	3.10	3.15	2.92	3.02
F	1.09	1.02	2.08	1.48	1.58	1.51	1.50	1.44	1.32	1.43	1.62	1.68	1.45	1.55	1.31	0.80	0.85	0.90	0.85	1.08	0.98
X_{Mg}	0.81	0.80	0.83	0.79	0.78	0.74	0.75	0.76	0.73	0.76	0.73	0.81	0.81	0.87	0.87	0.51	0.52	0.52	0.55	0.60	0.59
X_F	0.27	0.25	0.52	0.37	0.40	0.38	0.37	0.36	0.33	0.36	0.41	0.42	0.36	0.39	0.33	0.20	0.21	0.22	0.21	0.27	0.25

Table 5.2. Continued.

Sample	PLB2B											S26	17EG07								
Phase	Bt	Bt	Bt	Bt	Bt	Bt	Bt	Bt	Bt	Bt	Bt	Bt	Bt	Bt	Bt	Bt	Bt	Bt	Bt	Bt	Bt
Anal. no.	37	38	44	48	49	51	66	67	70	71	72	100	1	2	41	51	54	70	74	75	85
SiO_2	36.85	37.08	36.81	36.84	36.87	37.64	44.30	36.76	37.05	36.91	36.93	59.79	38.68	38.67	38.94	39.26	38.75	38.82	39.24	39.46	38.20
TiO_2	4.45	4.14	4.40	4.07	5.16	3.91	4.33	5.28	5.05	5.10	5.05	0.04	4.68	4.69	4.61	4.11	4.84	4.72	4.03	5.19	4.46
Al_2O_3	12.60	12.87	12.75	13.15	12.64	12.88	11.05	13.31	12.87	12.76	12.68	16.85	12.15	12.18	12.27	12.54	12.16	12.57	12.57	13.03	12.09
Cr_2O_3	0.04	0.04	0.01	0.02	0.06		0.06	0.06	0.04	0.04	0.01	0.02	0.02	0.03	0.04	0.04	0.03	0.04	0.04	0.04	0.04
FeO	17.63	17.37	18.31	17.23	17.75	16.57	16.64	17.91	17.90	17.93	17.95	4.98	11.52	11.74	10.94	10.76	12.67	11.47	9.73	9.13	11.98
MnO	0.04	0.01	0.02	0.01		0.04	0.04	0.01	0.02	0.01	0.03	0.02	0.02	0.02	0.01	0.01	0.00	0.03	0.01	0.00	0.01
MgO	13.31	13.72	13.07	13.57	12.81	13.68	10.86	12.69	13.20	12.74	12.73	1.50	16.71	16.57	16.88	16.64	15.64	16.90	18.18	17.37	16.29
CaO																					
ZnO	0.06	0.08	0.05	0.05	0.06	0.08	0.03	0.09	0.04	0.03	0.10		0.07	0.06	0.11	0.01	0.06	0.06	0.03	0.12	0.08
Na_2O	0.08	0.07	0.07	0.12	0.10	0.09	0.09	0.07	0.10	0.08	0.08	0.76	0.04	0.06	0.05	0.06	0.08	0.14	0.09	0.11	0.06
K_2O	8.28	8.60	8.50	8.17	8.51	8.39	7.20	8.43	8.75	8.55	8.39	12.19	9.09	9.32	9.07	9.31	9.17	8.85	9.00	8.80	8.99
P_2O_5		0.01		0.06	0.03	0.05	0.09			0.02		0.04	0.02	0.05	0.05	0.03		0.05			0.03
F	1.87	2.35	1.86	1.97	1.75	2.19	1.39	1.80	2.10	2.22	2.31		3.89	3.91	4.22	4.70	3.95	4.81	4.82	4.53	4.27
H_2O	3.00	2.80	3.02	2.97	3.08	2.88	3.42	3.08	2.95	2.86	2.81	4.48	2.14	2.14	2.00	1.77	2.11	1.74	1.75	1.92	1.92
Total	98.21	99.14	98.87	98.23	98.82	98.40	99.50	99.49	100.07	99.25	99.07	100.67	99.0348	99.4406	99.1902	99.2412	99.462	100.204	99.4862	99.6875	98.4193
O-basis												11									
Si	5.680	5.673	5.658	5.664	5.655	5.762	6.516	5.597	5.626	5.653	5.666	8.002	5.814	5.805	5.836	5.886	5.831	5.784	5.837	5.821	5.808
Ti	0.516	0.476	0.509	0.471	0.595	0.450	0.479	0.605	0.577	0.587	0.583	0.004	0.529	0.530	0.520	0.463	0.548	0.529	0.451	0.576	0.510
Al	2.289	2.321	2.310	2.383	2.285	2.324	1.916	2.389	2.304	2.303	2.293	2.658	2.153	2.155	2.168	2.216	2.157	2.208	2.204	2.265	2.167
Cr	0.005	0.005	0.001	0.002	0.007		0.007	0.007	0.005	0.005	0.001	0.002	0.002	0.004	0.005	0.005	0.004	0.005	0.005	0.005	0.005
Fe^{2+}	2.273	2.223	2.354	2.216	2.277	2.121	2.047	2.281	2.273	2.297	2.303	0.557	1.448	1.474	1.371	1.349	1.595	1.429	1.210	1.126	1.523
Mn	0.005	0.001	0.003	0.001		0.005	0.005	0.001	0.003	0.001	0.004	0.002	0.003	0.003	0.001	0.001		0.004	0.001		0.001
Mg	3.058	3.129	2.995	3.110	2.929	3.122	2.381	2.880	2.988	2.909	2.911	0.299	3.744	3.708	3.771	3.719	3.508	3.754	4.031	3.819	3.692
Ca																					
Zn	0.007	0.009	0.006	0.006	0.007	0.009	0.003	0.010	0.004	0.003	0.011		0.008	0.007	0.012	0.001	0.007	0.007	0.003	0.013	0.009
Na	0.024	0.021	0.021	0.036	0.030	0.027	0.026	0.021	0.029	0.024	0.024	0.197	0.012	0.017	0.015	0.017	0.005	0.006	0.007	0.009	0.000
K	1.628	1.678	1.666	1.602	1.665	1.638	1.351	1.637	1.695	1.670	1.642	2.081	1.743	1.785	1.734	1.780	1.760	1.682	1.707	1.656	1.744
Cation	15.484	15.537	15.522	15.491	15.451	15.458	14.731	15.429	15.505	15.453	15.437	13.803	15.456	15.487	15.432	15.439	15.414	15.407	15.456	15.290	15.459
OH*	3.09	2.86	3.10	3.04	3.15	2.94	3.35	3.13	2.99	2.92	2.88	4.00	2.15	2.14	2.00	1.77	2.12	1.73	1.73	1.89	1.95
F	0.91	1.14	0.90	0.96	0.85	1.06	0.65	0.87	1.01	1.08	1.12	0.00	1.85	1.86	2.00	2.23	1.88	2.27	2.27	2.11	2.05
X_{Mg}	0.57	0.58	0.56	0.58	0.56	0.60	0.54	0.56	0.57	0.56	0.56	0.35	0.72	0.72	0.73	0.73	0.69	0.72	0.77	0.77	0.71
X_F	0.23	0.28	0.23	0.24	0.21	0.27	0.16	0.22	0.25	0.27	0.28	0.00	0.46	0.46	0.50	0.56	0.47	0.57	0.57	0.53	0.51

Table 5.2. Continued.

Sample	17EG07			PLB7/2																		
Phase	Bt	Bt	Bt	Bt	Bt	Bt	Bt	Bt	Bt	Bt	Bt	Bt	Bt	Bt	Bt	Bt	Bt	Bt	Bt	Bt	Bt	Bt
Anal. no.	90	91	98	7	8	12	14	15	22	26	27	33	34	38	41	43	46	47	48	53	56	
SiO_2	38.43	36.36	37.00	36.00	36.69	36.53	36.39	37.05	36.35	36.65	37.10	36.27	36.28	35.64	36.10	36.61	36.13	36.07	36.72	36.32	36.78	
TiO_2	4.33	4.23	2.74	5.09	5.21	5.62	3.70	3.61	4.56	5.06	4.79	5.12	5.39	5.83	5.15	3.63	5.76	4.09	3.89	3.68	4.95	
Al_2O_3	12.15	11.17	10.94	12.97	12.69	12.66	12.93	12.85	11.99	12.92	12.91	13.01	13.10	12.64	13.02	13.46	12.84	13.22	13.22	12.85	12.55	
Cr_2O_3	0.02	0.04	0.04		0.02	0.06			0.03	0.05	0.02	0.03	0.02	0.03			0.01	0.02		0.04	0.02	
FeO	12.44	15.83	8.59	19.12	18.94	17.73	18.62	18.71	19.31	18.99	18.82	19.96	20.05	20.44	20.14	18.27	19.77	19.38	18.69	18.75	19.99	
MnO	0.01	0.02	0.01		0.01	0.01	0.02	0.01				0.00	0.01	0.03	0.03	0.01		0.01	0.02	0.02	0.02	
MgO	16.47	14.57	20.16	11.84	11.69	11.19	12.92	12.56	12.45	11.82	11.74	10.36	10.08	9.72	10.78	12.52	10.74	11.90	12.18	12.15	10.63	
CaO																						
ZnO	0.09	0.07	0.09	0.08	0.04	0.13	0.08	0.07	0.06	0.09	0.10	0.07	0.07	0.07	0.07	0.05	0.11	0.06	0.04	0.10	0.09	
Na_2O	0.06	0.06	0.01	0.04	0.05	0.05	0.02	0.04	0.06	0.08	0.06	0.08	0.05	0.07	0.06	0.04	0.07	0.08	0.08	0.04	0.04	
K_2O	9.12	7.76	9.14	8.82	8.67	7.98	8.70	8.89	8.76	8.80	8.80	8.67	8.55	8.75	8.79	8.80	8.97	8.87	8.95	8.99	9.01	
P_2O_5	0.02	0.09	0.09	0.01		0.04	0.01		0.02		0.01			0.06		0.01	0.04		0.04	0.02		
F	4.48	3.79	5.29	1.71	2.06	1.86	2.23	1.53	2.34	1.98	1.75	1.84	1.83	1.34	2.06	1.93	1.02	1.78	2.44	1.67	1.67	
H_2O	1.85	1.99	1.33	3.06	2.91	2.95	2.80	3.16	2.74	2.96	3.07	2.97	2.98	3.17	2.88	2.96	3.39	3.01	2.72	3.04	3.07	
Total	99.4695	95.9794	95.4259	98.7383	98.9789	96.8136	98.4244	98.4756	98.6689	99.4008	99.1747	98.3828	98.4112	97.7935	99.0834	98.2885	98.8482	98.4908	98.9913	97.6704	98.8191	
O-basis				11	11	11	11	11	11	11	11	11	11	11	11	11	11	11	11	11	11	
Si	5.799	5.758	5.787	5.579	5.662	5.711	5.651	5.724	5.664	5.636	5.698	5.656	5.652	5.611	5.608	5.667	5.596	5.611	5.678	5.683	5.712	
Ti	0.491	0.504	0.322	0.593	0.605	0.661	0.432	0.419	0.534	0.585	0.553	0.600	0.632	0.690	0.602	0.423	0.671	0.478	0.452	0.433	0.578	
Al	2.161	2.085	2.017	2.369	2.308	2.333	2.367	2.340	2.202	2.342	2.337	2.391	2.406	2.346	2.384	2.456	2.344	2.424	2.409	2.370	2.297	
Cr	0.002	0.005	0.005		0.002	0.007			0.004	0.006	0.002	0.004	0.002	0.004			0.001	0.002		0.005	0.002	
Fe^{2+}	1.570	2.097	1.124	2.478	2.444	2.318	2.418	2.418	2.516	2.442	2.417	2.603	2.612	2.691	2.617	2.365	2.561	2.521	2.417	2.454	2.597	
Mn	0.001	0.003	0.001		0.001	0.001	0.003	0.001			0.001		0.001	0.004	0.004	0.001	0.000	0.001	0.003	0.003	0.003	
Mg	3.705	3.440	4.700	2.735	2.689	2.608	2.991	2.893	2.892	2.709	2.688	2.408	2.341	2.281	2.496	2.889	2.480	2.760	2.807	2.834	2.461	
Ca																						
Zn	0.010	0.008	0.010	0.009	0.005	0.015	0.009	0.008	0.007	0.010	0.011	0.008	0.008	0.008	0.008	0.006	0.013	0.007	0.005	0.012	0.010	
Na	0.018	0.018	0.003	0.012	0.015	0.015	0.006	0.012	0.018	0.024	0.018	0.024	0.015	0.021	0.018	0.012	0.021	0.024	0.024	0.012	0.012	
K	1.755	1.568	1.823	1.744	1.707	1.591	1.723	1.752	1.741	1.726	1.724	1.725	1.699	1.757	1.742	1.738	1.772	1.760	1.765	1.794	1.785	
Cation	15.514	15.486	15.793	15.520	15.439	15.261	15.599	15.568	15.578	15.480	15.450	15.420	15.369	15.413	15.478	15.557	15.457	15.589	15.560	15.600	15.458	
OH*	1.86	2.10	1.38	3.16	2.99	3.08	2.90	3.25	2.85	3.04	3.15	3.09	3.10	3.33	2.99	3.06	3.50	3.12	2.81	3.17	3.18	
F	2.14	1.90	2.62	0.84	1.01	0.92	1.10	0.75	1.15	0.96	0.85	0.91	0.90	0.67	1.01	0.94	0.50	0.88	1.19	0.83	0.82	
X_{Mg}	0.70	0.62	0.81	0.52	0.52	0.53	0.55	0.54	0.53	0.53	0.53	0.48	0.47	0.46	0.49	0.55	0.49	0.52	0.54	0.54	0.49	
X_F	0.53	0.47	0.65	0.21	0.25	0.23	0.27	0.19	0.29	0.24	0.21	0.23	0.23	0.17	0.25	0.24	0.12	0.22	0.30	0.21	0.21	

Table 5.2. Continued.

Sample	PLB7/2				PLB89A								
Phase	Bt	Bt	Bt	Bt	Bt	Bt	Bt	Bt	Bt	Bt	Bt	Bt	Bt
Anal. no.	57	63	64	65	2	11	12	15	21	38	39	47	51
SiO_2	35.80	36.62	37.09	37.08	35.55	36.03	36.95	35.97	35.55	35.49	35.62	35.57	35.85
TiO_2	5.11	4.74	4.39	5.09	5.12	5.64	5.45	3.30	5.57	5.35	4.98	5.78	4.96
Al_2O_3	12.70	12.79	12.83	13.22	13.75	13.75	12.54	14.39	13.58	13.71	14.09	13.81	13.81
Cr_2O_3	0.04	0.02	0.02	0.05	0.03	0.01	0.02	0.04	0.01	0.05	0.01	0.01	0.05
FeO	19.97	17.31	17.45	16.33	22.30	22.07	21.87	21.46	22.02	22.42	21.76	22.21	22.12
MnO	0.02			0.01	0.03	0.02	0.04	0.03	0.01	0.03	0.03	0.03	0.04
MgO	10.52	12.28	12.73	12.72	8.24	8.48	8.59	9.87	8.49	8.14	8.67	8.22	8.71
CaO							0.05	0.07					
ZnO	0.09	0.09	0.10	0.02	0.10	0.09	0.12	0.09	0.06	0.08	0.08	0.05	0.10
Na_2O	0.05	0.07	0.02	0.02	0.30	0.13	0.31	0.27	0.06	0.15	0.06	0.23	0.12
K_2O	8.93	8.88	9.02	8.79	8.33	8.70	8.09	8.15	8.77	8.72	8.68	8.68	8.63
P_2O_5			0.01		0.01	0.03	0.10	0.04		0.05	0.01	0.06	0.04
F	1.67	2.27	1.96	1.65	0.35	0.44	0.55	0.65	0.62	0.44	0.36	0.36	0.40
H_2O	3.02	2.78	2.97	3.13	3.64	3.65	3.58	3.53	3.53	3.61	3.66	3.67	3.65
Total	97.9241	97.8529	98.5858	98.1094	97.60	98.83	97.93	97.54	98.01	98.00	97.85	98.47	98.27
O-basis	11	11	11	11	11	11	11	11	11	11	11	11	11
Si	5.626	5.690	5.710	5.684	5.595	5.593	5.764	5.625	5.575	5.577	5.579	5.553	5.600
Ti	0.604	0.554	0.508	0.587	0.606	0.658	0.639	0.388	0.657	0.632	0.587	0.679	0.583
Al	2.352	2.342	2.328	2.389	2.551	2.516	2.306	2.652	2.510	2.539	2.601	2.541	2.543
Cr	0.005	0.002	0.002	0.006	0.004	0.001	0.002	0.005	0.001	0.006	0.001	0.001	0.006
Fe^{2+}	2.625	2.249	2.247	2.094	2.935	2.865	2.853	2.807	2.888	2.946	2.850	2.900	2.890
Mn	0.003			0.001	0.004	0.003	0.005	0.004	0.001	0.004	0.004	0.004	0.005
Mg	2.464	2.844	2.921	2.907	1.933	1.962	1.998	2.301	1.985	1.907	2.024	1.913	2.028
Ca							0.008	0.012					
Zn	0.010	0.010	0.011	0.002	0.012	0.010	0.014	0.010	0.007	0.009	0.009	0.006	0.012
Na	0.015	0.021	0.006	0.006	0.092	0.039	0.094	0.082	0.018	0.046	0.018	0.070	0.036
K	1.790	1.760	1.771	1.719	1.672	1.723	1.610	1.626	1.754	1.748	1.734	1.729	1.719
Cation	15.494	15.474	15.505	15.394	15.404	15.371	15.294	15.512	15.398	15.415	15.409	15.396	15.421
OH*	3.17	2.88	3.05	3.20	3.83	3.78	3.73	3.68	3.69	3.78	3.82	3.82	3.80
F	0.83	1.12	0.95	0.80	0.17	0.22	0.27	0.32	0.31	0.22	0.18	0.18	0.20
X_{Mg}	0.48	0.56	0.57	0.58	0.40	0.41	0.41	0.45	0.41	0.39	0.42	0.40	0.41
X_F	0.21	0.28	0.24	0.20	0.04	0.05	0.07	0.08	0.08	0.05	0.04	0.04	0.05

Table 5.2. Continued.

Sample	17EG18B		S26													17EG07			
Phase	Opx	Opx	Opx	Opx	Opx	Opx	Opx	Opx	Opx	Opx	Opx	Opx	Opx	Opx	Opx	Opx	Opx	Opx	Opx
Anal. no.	21	62	43	44	46	49	63	65	76	81	92	94	98	101	111	15	16	19	37
SiO_2	49.48	49.63	50.11	49.74	49.93	50.25	48.89	50.08	43.82	50.44	51.2	50.1	49.53	51.42	50.39	50.2	50.4	50.09	50.17
TiO_2	0.13	0.13	0.12	0.12	0.10	0.08	0.09	0.08	5.95	0.11	0.11	0.13	0.07	0.08	0.10	0.11	0.08	0.09	0.10
Al_2O_3	4.78	4.4	1.91	1.79	1.52	1.59	1.61	1.52	2.00	1.69	1.51	1.93	1.61	1.30	1.37	1.07	0.96	1.40	1.85
Cr_2O_3	0.03	0.04			0.03	0.02	0.02	0.03	0.02	0.01		0.02	0.02	0.03		0.02	0.01	0.05	0.01
Fe_2O_3	0.65	1.39	0.00	0.69	0.60	1.06	3.02	1.44		1.34		1.58	2.20		0.63				
FeO	25.62	24.00	29.50	28.27	29.40	28.35	27.83	29.07	28.85	27.33	29.72	30.01	28.90	31.43	30.85	32.74	32.60	33.69	31.60
MnO	0.22	0.23	0.25	0.28	0.26	0.27	0.28	0.27	0.23	0.27	0.28	0.29	0.24	0.26	0.31	0.25	0.24	0.23	0.26
MgO	18.53	19.58	16.5	17.17	16.67	17.44	16.83	16.92	16.72	18.19	16.81	16.34	16.65	16.47	16.24	14.76	14.99	14.12	15.45
CaO	0.25	0.23	0.45	0.39	0.36	0.36	0.37	0.35	0.29	0.3	0.34	0.39	0.36	0.36	0.3	0.57	0.57	0.69	0.49
Na_2O	0.02		0.01			0.01	0.01	0.02	0.06	0.02	0.01	0.02		0.01		0.02	0.01		0.01
K_2O		0.01							0.03										
Total	99.71	99.64	99.02	98.45	98.87	99.43	98.95	99.78	97.97	99.69	99.98	100.81	99.58	101.36	100.19	99.74	99.86	100.36	99.94
O-basis	6	6	6	6	6	6	6	6	6	6	6	6	6	6	6	6	6	6	6
Si	1.880	1.878	1.953	1.944	1.952	1.946	1.915	1.941	1.746	1.939	1.977	1.930	1.929	1.983	1.955	1.985	1.995	2.022	1.963
Ti	0.004	0.004	0.004	0.004	0.003	0.002	0.003	0.002	0.178	0.003	0.003	0.004	0.002	0.002	0.003	0.003	0.002	0.003	0.003
Al	0.214	0.196	0.088	0.082	0.070	0.073	0.074	0.069	0.094	0.077	0.069	0.088	0.074	0.059	0.063	0.050	0.045	0.067	0.085
Cr	0.001	0.001			0.001	0.001	0.001	0.001	0.001	0.000	0.000	0.001	0.001	0.001		0.001		0.002	
Fe^{3+}	0.019	0.040		0.020	0.018	0.031	0.089	0.042	0.063	0.039	0.000	0.046	0.064		0.018	0.000			
Fe^{2+}	0.814	0.760	0.966	0.924	0.961	0.918	0.912	0.942	0.899	0.879	0.960	0.967	0.941	0.984	1.001	1.057	1.040	1.020	1.017
Mn	0.007	0.007	0.008	0.009	0.009	0.009	0.009	0.009	0.008	0.009	0.009	0.009	0.008	0.008	0.010	0.008	0.008	0.008	0.009
Mg	1.050	1.105	0.958	1.001	0.972	1.007	0.983	0.978	0.993	1.042	0.968	0.938	0.966	0.947	0.939	0.870	0.885	0.850	0.901
Ca	0.010	0.009	0.019	0.016	0.015	0.015	0.016	0.015	0.012	0.012	0.014	0.016	0.015	0.015	0.012	0.024	0.024	0.030	0.021
Zn																			
Na	0.001		0.001			0.001	0.001	0.002	0.005	0.001	0.001	0.001		0.001		0.002	0.001		0.001
K									0.002										
Cation	4	4	4	4	4	4	4	4	4	4	4	4	4	4	4	4	4	4	4
X_{Mg}	0.56	0.59	0.50	0.52	0.50	0.52	0.52	0.51	0.52	0.54	0.50	0.49	0.51	0.49	0.48	0.45	0.46	0.45	0.47
X_{En}	0.56	0.59	0.49	0.52	0.50	0.52	0.51	0.51	0.52	0.54	0.49	0.49	0.50	0.48	0.48	0.44	0.44	0.42	0.46
X_{Fs}	0.43	0.41	0.50	0.48	0.49	0.47	0.48	0.49	0.47	0.45	0.50	0.50	0.49	0.51	0.51	0.55	0.54	0.56	0.53

Table 5.2. Continued.

Sample	17EG07				PLB2B														
Phase	Opx	Opx	Opx	Opx	Opx	Opx	Opx	Opx	Opx	Opx	Opx	Opx	Opx	Opx	Opx	Opx	Opx	Opx	Opx
Anal. no.	39	47	82	94	17	18	19	20	22	23	24	26	27	28	53	54	55	64	65
SiO_2	49.85	50.52	50.26	50.22	49.31	48.62	49.1	49.43	50.03	49.69	49.43	49.02	49.37	49.78	50.05	49.41	49.97	49.65	48.85
TiO_2	0.34	0.12	0.08	0.11	0.06	0.31	0.07	0.07	0.08	0.14	0.17	0.58	0.05	0.23	0.05	0.47	0.07	0.17	0.08
Al_2O_3	1.10	1.02	1.05	1.14	1.17	1.79	1.30	1.35	0.89	0.78	1.33	1.21	1.57	0.91	1.02	1.14	1.01	1.13	1.16
Cr_2O_3	0.03	0.02	0.01	0.01		0.02	0.03	0.02	0.02	0.03	0.04	0.04	0.03	0.02	0.02	0.03	0.02	0.02	0.02
Fe_2O_3					1.43	2.67	1.53	1.24	1.60	2.28	2.13	2.10	2.02	2.08	1.22	1.72	1.39	1.58	3.21
FeO	33.59	31.71	32.11	32.12	33.62	32.11	33.19	33.71	32.96	32.17	32.45	32.39	32.36	31.92	31.96	31.73	31.45	32.12	30.58
MnO	0.31	0.28	0.22	0.22	0.7	0.67	0.59	0.58	0.57	0.58	0.54	0.45	0.44	0.37	0.33	0.37	0.32	0.42	0.37
MgO	14.17	15.52	15.17	15.19	13.52	13.38	13.57	13.51	14.3	14.58	14.27	14.31	14.37	14.91	15.04	14.93	15.3	14.67	15.05
CaO	0.59	0.60	0.6	0.57	0.36	0.35	0.51	0.54	0.57	0.55	0.6	0.54	0.51	0.6	0.48	0.54	0.54	0.61	0.55
Na_2O		0.02			0.02	0.01	0.03	0.02	0.03	0.02	0.00	0.02		0.02	0.03	0.02	0.01	0.01	
K_2O			0.01		0.01	0.42					0.02				0.01		0.01		
Total	99.98	99.81	99.51	99.58	100.20	100.35	99.92	100.47	101.05	100.82	100.97	100.66	100.72	100.84	100.21	100.36	100.09	100.38	99.87
O-basis	6	6	6	6	6	6	6	6	6	6	6	6	6	6	6	6	6	6	6
Si	1.994	1.983	1.990	1.982	1.951	1.920	1.945	1.949	1.954	1.945	1.933	1.924	1.932	1.942	1.958	1.935	1.955	1.946	1.923
Ti	0.010	0.004	0.002	0.003	0.002	0.009	0.002	0.002	0.002	0.004	0.005	0.017	0.001	0.007	0.001	0.014	0.002	0.005	0.002
Al	0.052	0.047	0.049	0.053	0.055	0.083	0.061	0.063	0.041	0.036	0.061	0.056	0.072	0.042	0.047	0.053	0.047	0.052	0.054
Cr	0.001	0.001				0.001	0.001	0.001	0.001	0.001	0.001	0.001	0.001	0.001	0.001	0.001	0.001	0.001	0.001
Fe^{3+}					0.043	0.079	0.046	0.037	0.047	0.067	0.063	0.062	0.059	0.061	0.036	0.051	0.041	0.047	0.095
Fe^{2+}	1.062	1.021	1.029	1.037	1.112	1.061	1.100	1.112	1.077	1.053	1.061	1.063	1.059	1.041	1.046	1.039	1.029	1.053	1.007
Mn	0.011	0.009	0.007	0.007	0.023	0.022	0.020	0.019	0.019	0.019	0.018	0.015	0.015	0.012	0.011	0.012	0.011	0.014	0.012
Mg	0.845	0.908	0.896	0.894	0.797	0.788	0.802	0.794	0.833	0.851	0.832	0.837	0.838	0.867	0.877	0.872	0.892	0.857	0.883
Ca	0.025	0.025	0.025	0.024	0.015	0.015	0.022	0.023	0.024	0.023	0.025	0.023	0.021	0.025	0.020	0.023	0.023	0.026	0.023
Zn																			
Na		0.002			0.002	0.001	0.002	0.002	0.002	0.002		0.002		0.002	0.002	0.002	0.001	0.001	
K			0.001		0.001	0.021					0.001								
Cation	4	4	4	4	4	4	4	4	4	4	4	4	4	4	4	4	4	4	4
X_{Mg}	0.44	0.47	0.47	0.46	0.42	0.43	0.42	0.42	0.44	0.45	0.44	0.44	0.44	0.45	0.46	0.46	0.46	0.45	0.47
X_{En}	0.42	0.46	0.45	0.45	0.41	0.42	0.42	0.41	0.43	0.44	0.43	0.44	0.44	0.45	0.45	0.45	0.46	0.44	0.46
X_{Fs}	0.56	0.53	0.54	0.54	0.58	0.57	0.57	0.58	0.56	0.55	0.55	0.55	0.55	0.54	0.54	0.54	0.53	0.54	0.53

Table 5.2. Continued.

Sample	17EG18B						S26												17EG07	
Phase	Ilm	Ilm	Ilm	Ilm	Ilm	Ilm	Ilm	Ilm	Ilm	Ilm	Ilm	Ilm	Ilm	Ilm	Ilm	Ilm	Ilm	Ilm	Ilm	Ilm
Anal. no.	10	13	14	33	34	57	4	10	18	32	56	74	77	80	86	103	104	107	25	27
SiO_2	0.09	0.09	0.11				0.01	0.17	0.2	0.03	0.03	0.07	0.03	0.02	0.05	0.03	0.02	0.02	0.06	0.02
TiO_2	50.91	47.24	47.1	45.11	44.79	47.04	51.61	51.39	51.72	50.92	51.47	50.73	51.18	50.84	51.24	51.05	51.01	51.23	51.23	51.29
Al_2O_3	0.06	0.09	0.09	0.05	0.04	0.07	0.06	0.08	0.15	0.07	0.05	0.11	0.06	0.06	0.11	0.06	0.04	0.03	0.10	0.08
Cr_2O_3	0.04	0.05	0.06	0.06	0.07	0.04	0.05	0.03	0.01	0.05	0.03	0.02	0.05	0.02	0.03	0.06	0.01	0.04	0.05	0.03
Fe_2O_3	0.75	6.95	7.05	11.85	12.47	7.89	1.48	0.34		1.92	1.43	2.54	1.91	1.82	1.55	2.71	2.73	2.00		0.19
FeO	44.66	41.56	41.34	39.60	39.33	40.45	44.13	45.36	45.35	44.06	43.98	42.74	43.62	43.33	43.74	43.94	43.89	44.25	44.05	44.14
MnO	0.14	0.02	0.03	0.14	0.14	0.13	0.22	0.25	0.43	0.28	0.21	0.19	0.23	0.21	0.16	0.20	0.26	0.27	0.19	0.22
MgO	0.61	0.58	0.61	0.46	0.46	0.62	1.17	0.42	0.1	0.84	1.18	1.54	1.25	1.23	1.27	1.01	0.96	0.88	0.62	0.97
CaO	0.01		0.03	0.01		0.49		0.05	0.03		0.03	0.03		0.01		0.01	0.03	0.01	0.07	0.05
ZnO	0.08	0.01		0.04		0.08	0.04	0.03		0.01	0.03	0.06	0.14		0.02	0.12	0.04			0.02
Total	97.22	96.52	96.36	97.23	97.23	96.66	98.68	98.06	97.98	98.11	98.37	97.94	98.27	97.54	98.17	99.19	98.99	98.73	96.37	97.01
O-basis	4	4	4	4	4	4	4	4	4	4	4	4	4	4	4	4	4	4	4	4
Si	0.002	0.002	0.003					0.004	0.005	0.001	0.001	0.002	0.001	0.001	0.001	0.001	0.001	0.001	0.002	0.001
Ti	0.988	0.927	0.926	0.882	0.876	0.920	0.984	0.990	1.001	0.979	0.984	0.971	0.978	0.981	0.982	0.971	0.972	0.980	1.004	0.996
Al	0.002	0.003	0.003	0.002	0.001	0.002	0.002	0.002	0.005	0.002	0.001	0.003	0.002	0.002	0.003	0.002	0.001	0.001	0.003	0.002
Cr	0.001	0.001	0.001	0.001	0.001	0.001	0.001	0.001		0.001	0.001		0.001		0.001	0.001		0.001	0.001	0.001
Fe^{3+}	0.016	0.137	0.139	0.233	0.245	0.156	0.029	0.007		0.037	0.028	0.050	0.039	0.035	0.030	0.054	0.053	0.038	0.000	0.004
Fe^{2+}	0.962	0.907	0.903	0.860	0.855	0.878	0.934	0.971	0.992	0.941	0.934	0.909	0.924	0.929	0.931	0.927	0.929	0.941	0.976	0.952
Mn	0.003	0.000	0.001	0.003	0.003	0.003	0.005	0.005	0.009	0.006	0.005	0.004	0.005	0.005	0.003	0.004	0.006	0.006	0.004	0.005
Mg	0.023	0.023	0.024	0.018	0.018	0.024	0.044	0.016	0.004	0.032	0.045	0.058	0.047	0.047	0.048	0.038	0.036	0.033	0.024	0.037
Ca			0.001			0.014		0.001	0.001		0.001	0.001				0.000	0.001		0.002	0.001
Zn	0.002			0.001		0.002	0.001	0.001			0.001	0.001	0.003			0.002	0.001			
Cation	2	2	2	2	2	2	2	2	2	2	2	2	2	2	2	2	2	2	2	2
X^{Fe3+}	0.01	0.14	0.13	0.21	0.22	0.15	0.03	0.01	0.00	0.04	0.03	0.05	0.04	0.04	0.03	0.05	0.05	0.04	0.00	0.00
X_{Hem}	0.01	0.07	0.07	0.12	0.12	0.08	0.01	0.00	0.00	0.02	0.01	0.03	0.02	0.02	0.02	0.03	0.03	0.02	0.00	0.00
X_{Gk}	0.02	0.02	0.02	0.02	0.02	0.02	0.04	0.02	0.00	0.03	0.05	0.06	0.05	0.05	0.05	0.04	0.04	0.03	0.02	0.04
X_{Ilm}	0.97	0.91	0.91	0.86	0.86	0.90	0.94	0.98	1.00	0.95	0.94	0.92	0.93	0.93	0.94	0.93	0.94	0.95	0.98	0.96

Table 5.2. Continued.

Sample	17EG07							PLB2B				PLB89A
Phase	Ilm	Ilm	Ilm	Ilm	Ilm	Ilm	Ilm	Ilm	Ilm	Ilm	Ilm	Ilm
Anal. no.	38	44	46	57	63	68	78	7	21	33	46	37
SiO_2	0.02	0.01	0.01	0.03	0.02	0.04	0.04	0.06	0.18	0.05	0.05	0.01
TiO_2	51.38	51.57	51.49	50.76	51.59	51.21	51.25	50.18	49.85	48.77	49.22	49.01
Al_2O_3	0.06	0.05	0.06	0.06	0.05	0.06	0.09	0.21	0.11	0.08	0.19	0.05
Cr_2O_3	0.08	0.02	0.08	0.06	0.04	0.06	0.03	0.02	0.02	0.03	0.02	0.01
Fe_2O_3	1.06	0.64	0.45	1.79	0.77	1.48	0.87	2.27	2.93	5.84	5.43	4.35
FeO	44.65	44.48	44.32	43.97	44.65	43.76	43.91	44.21	43.99	43.23	43.50	43.62
MnO	0.23	0.2	0.23	0.19	0.21	0.18	0.19	0.59	0.43	0.24	0.23	0.33
MgO	0.77	0.94	1.01	0.85	0.88	1.20	1.13	0.19	0.34	0.22	0.33	0.08
CaO		0.03		0.01		0.02	0.02	0.05	0.02	0.05	0.01	
ZnO	0.07	0.08	0.06		0.02		0.07	0.02	0.02	0.03	0.05	0.01
Total	98.32	98.02	97.70	97.72	98.23	98.01	97.61	97.80	97.88	98.53	99.02	97.47
O-basis	4	4	4	4	4	4	4	4	4	4	4	4
Si	0.001			0.001	0.001	0.001	0.001	0.002	0.005	0.001	0.001	
Ti	0.987	0.992	0.993	0.980	0.991	0.983	0.988	0.973	0.965	0.940	0.943	0.956
Al	0.002	0.002	0.002	0.002	0.002	0.002	0.003	0.006	0.003	0.002	0.006	0.002
Cr	0.002		0.002	0.001	0.001	0.001	0.001			0.001		
Fe^{3+}	0.022	0.014	0.010	0.035	0.015	0.029	0.018	0.045	0.057	0.113	0.105	0.085
Fe^{2+}	0.952	0.949	0.949	0.944	0.953	0.934	0.940	0.952	0.946	0.926	0.926	0.946
Mn	0.005	0.004	0.005	0.004	0.005	0.004	0.004	0.013	0.009	0.005	0.005	0.007
Mg	0.029	0.036	0.039	0.033	0.033	0.046	0.043	0.007	0.013	0.008	0.013	0.003
Ca		0.001				0.001	0.001	0.001	0.001	0.001		
Zn	0.001	0.002	0.001				0.001			0.001	0.001	
Cation	2	2	2	2	2	2	2	2	2	2	2	2
X^{Fe3+}	0.02	0.01	0.01	0.04	0.02	0.03	0.02	0.04	0.06	0.11	0.10	0.08
X_{Hem}	0.01	0.01	0.01	0.02	0.01	0.01	0.01	0.02	0.03	0.06	0.05	0.04
X_{Gk}	0.03	0.04	0.04	0.03	0.03	0.05	0.04	0.01	0.01	0.01	0.01	0.00
X_{Ilm}	0.96	0.96	0.96	0.95	0.96	0.94	0.95	0.97	0.96	0.93	0.93	0.95

Table 5.2. Continued.

Sample	17EG18B							PLB2B												
Phase	Kfs	Kfs	Kfs	Kfs	Kfs	Kfs	Kfs	Pl	Pl	Pl	Pl	Pl	Pl	Pl	Pl	Pl	Pl	Pl	Pl	Pl
Anal. no.	8	9	25	29	31	37	60	22	40	48	49	1	2	14	16	25	30	45	47	60
SiO_2	64.68	64.6	63.83	64.78	64.45	64.29	64.85	54.48	54.71	54.11	54.1	53.85	52.9	54.55	68.58	55.38	55.36	55.49	54.34	49.44
TiO_2	0.05	0.03	0.05	0.03	0.04	0.01	0.03	0.02			0.03	0.01	0.02	0.03					0.03	0.02
Al_2O_3	19.27	19.3	19.48	19.3	19.18	19.47	19.42	28.51	28.45	28.54	28.69	27.81	27.74	27.5	19.03	27.3	27.6	27.05	27.85	25.9
Cr_2O_3	0.01	0.01	0.48	0.01	0.03	0.03	0.07	0.14	0.06	0.17	0.21	0.06	0.09	0.15	0.07	0.11	0.17	0.14	0.45	0.20
FeO	0.01	0.01	0.48	0.01	0.03	0.03	0.07	0.14	0.06	0.17	0.21	0.06	0.09	0.15	0.07	0.11	0.17	0.14	0.45	0.20
MnO			0.01					0.02		0.01	0.02	0.02	0.01			0.01			0.01	0.02
MgO									0.01	0.01	0.01	0.02		0.02		0.02	0.01	0.02	0.14	0.04
CaO								11.44	11.65	11.61	11.51	11.57	12.17	11.67	7.12	11.58	11.72	11.17	11.28	14.49
ZnO	0.01	0.02	0.01					0.02	0.03				0.03		0.01			0.06	0.06	
Na_2O	2.18	2.21	2.09	2.37	2.24	2.11	2.64	4.84	4.6	4.87	4.74	4.89	4.61	4.89	4.18	4.75	4.66	4.86	4.78	4.66
K_2O	13.39	13.44	13.7	13.36	13.5	13.4	13.82	0.10	0.06	0.08	0.10	0.11	0.14	0.15	0.05	0.19	0.12	0.15	0.16	0.15
P_2O_5	0.09	0.07	0.05	0.12	0.05	0.09	0.08	0.02	0.06	0.03	0.11	0.04	0.06	0.04	0.04	0.07	0.09	0.05		3.79
Total	99.69	99.69	100.18	99.98	99.52	99.43	100.98	99.73	99.69	99.6	99.73	98.44	97.86	99.15	99.15	99.52	99.9	99.13	99.55	98.91
O-basis	8	8	8	8	8	8	8	8	8	8	8									
Si	2.968	2.966	2.944	2.965	2.967	2.959	2.953	2.468	2.474	2.458	2.453	2.468	2.452	2.490	3.005	2.508	2.505	2.523	2.474	2.381
Ti	0.002	0.001	0.002	0.001	0.001		0.001	0.001			0.001		0.001	0.001					0.001	0.001
Al	1.042	1.044	1.059	1.041	1.041	1.056	1.042	1.522	1.516	1.528	1.534	1.503	1.516	1.480	0.983	1.457	1.472	1.450	1.494	1.470
Fe^{2+}			0.019		0.001	0.001	0.003	0.005	0.002	0.006	0.008	0.002	0.003	0.006	0.003	0.004	0.006	0.005	0.017	0.008
Mn								0.001			0.001	0.001								0.001
Mg									0.001	0.001	0.001	0.001		0.001		0.001	0.001	0.001	0.010	0.003
Ca								0.555	0.564	0.565	0.559	0.568	0.604	0.571	0.334	0.562	0.568	0.544	0.550	0.748
Zn		0.001						0.001	0.001				0.001			0.000	0.000	0.002	0.002	0.000
Na	0.194	0.197	0.187	0.210	0.200	0.188	0.233	0.425	0.403	0.429	0.417	0.435	0.414	0.433	0.355	0.417	0.409	0.429	0.422	0.435
K	0.784	0.787	0.806	0.780	0.793	0.787	0.803	0.006	0.003	0.005	0.006	0.006	0.008	0.009	0.003	0.011	0.007	0.009	0.009	0.009
Cation	4.99	5.00	5.02	5.00	5.00	4.99	5.03	4.98	4.97	4.99	4.98	4.98	5.00	4.99	4.68	4.96	4.97	4.96	4.98	5.06
X_{Or}	0.80	0.80	0.81	0.79	0.80	0.81	0.77	0.01	0.00	0.00	0.01	0.01	0.01	0.01	0.00	0.01	0.01	0.01	0.01	0.01
X_{Ab}	0.20	0.20	0.19	0.21	0.20	0.19	0.23	0.43	0.42	0.43	0.42	0.43	0.40	0.43	0.51	0.42	0.42	0.44	0.43	0.37
X_{An}	0.00	0.00	0.00	0.00	0.00	0.00	0.00	0.56	0.58	0.57	0.57	0.56	0.59	0.56	0.48	0.57	0.58	0.55	0.56	0.63

Table 5.2. Continued.

Sample	PLB2B					S26														
Phase	Pl	Pl	Kfs	Kfs	Kfs	Pl	Pl	Pl	Pl	Pl	Pl	Pl	Pl	Pl	Pl	Pl	Pl	Pl	Pl	Pl
Anal. no.	61	63	15	59	62	7	14	20	22	23	25	27	37	59	67	69	82	88	90	91
SiO_2	69.06	55.1	64.46	64.56	64.46	61.98	54.32	54.02	54.88	61.47	61.57	54.71	54.38	55.16	54.32	54.56	54.76	54.74	56.17	76.43
TiO_2		0.01	0.03	0.03	0.01	0.03	0.02					0.01		0.02				0.01		
Al_2O_3	18.74	28	19.46	18.77	19.59	22.47	26.6	27.43	27.16	23.41	22.93	27.16	27.16	27.36	27.05	27.23	26.85	27.45	26.48	14.59
Cr_2O_3	0.02	0.08	0.04	0.07	0.07	1.08	0.77	0.31	0.06	0.1	0.25	0.07	0.04	0.24	0.44	0.06	0.55	0.04	0.32	0.32
FeO	0.02	0.08	0.04	0.07	0.07	1.08	0.77	0.31	0.06	0.1	0.25	0.07	0.04	0.24	0.44	0.06	0.55	0.04	0.32	0.32
MnO					0.02		0.01						0.01					0.01		
MgO						0.29	0.45	0.06	0.01	0.04	0.06	0.02	0	0.07	0.11	0.04	0.13		0.14	0.08
CaO	6.73	11.63				8.04	9.3	10.54	10.32	9.36	8.76	10.36	10.05	9.52	9.91	10.38	9.89	10.07	10.04	5.19
ZnO	0.02		0.01	0.03	0.05		0.06	0.04	0.04										0.07	0.01
Na_2O	3.93	4.74	1.27	2.1	2.44	4.78	5.42	5.24	5.5	4.37	4.27	5.38	5.32	5.39	5.24	5.24	5.43	5.36	5.01	3.21
K_2O	0.36	0.12	13.1	13.19	13.37	0.18	0.37	0.21	0.14	0.07	0.09	0.18	0.16	0.42	0.10	0.16	0.15	0.12	0.09	0.06
P_2O_5	0.03		0.08	0.03	0.03	0.07	0.03				0.08	0.07				0.12			0.04	0.06
Total	98.91	99.76	98.49	98.85	100.11	100.00	98.12	98.16	98.17	98.92	98.26	98.03	97.16	98.42	97.61	97.85	98.31	97.84	98.68	100.27
O-basis						8	8	8	8	8	8	8	8	8	8	8	8	8	8	8
Si	3.025	2.487	2.981	2.987	2.954	2.777	2.518	2.492	2.518	2.751	2.772	2.514	2.518	2.526	2.517	2.510	2.525	2.515	2.561	3.254
Ti			0.001	0.001		0.001	0.001							0.001						
Al	0.968	1.490	1.061	1.024	1.058	1.186	1.453	1.492	1.469	1.235	1.217	1.471	1.482	1.477	1.477	1.476	1.459	1.487	1.423	0.732
Fe^{2+}	0.001	0.003	0.002	0.003	0.003	0.040	0.030	0.012	0.002	0.004	0.009	0.003	0.002	0.009	0.017	0.002	0.021	0.002	0.012	0.011
Mn					0.001															
Mg						0.019	0.031	0.004	0.001	0.003	0.004	0.001		0.005	0.008	0.003	0.009		0.010	0.005
Ca	0.316	0.562				0.386	0.462	0.521	0.507	0.449	0.423	0.510	0.499	0.467	0.492	0.512	0.489	0.496	0.491	0.237
Zn	0.001			0.001	0.002		0.002	0.001	0.001										0.002	
Na	0.334	0.415	0.114	0.188	0.217	0.415	0.487	0.469	0.489	0.379	0.373	0.479	0.478	0.479	0.471	0.467	0.485	0.478	0.443	0.265
K	0.020	0.007	0.773	0.778	0.781	0.010	0.022	0.012	0.008	0.004	0.005	0.011	0.009	0.025	0.006	0.009	0.009	0.007	0.005	0.003
Cation	4.66	4.96	4.93	4.98	5.02	4.84	5.01	5.00	5.00	4.82	4.80	4.99	4.99	4.99	4.99	4.98	5.00	4.98	4.95	4.51
X_{Or}	0.03	0.01	0.87	0.81	0.78	0.01	0.02	0.01	0.01	0.00	0.01	0.01	0.01	0.03	0.01	0.01	0.01	0.01	0.01	0.01
X_{Ab}	0.50	0.42	0.13	0.19	0.22	0.51	0.50	0.47	0.49	0.46	0.47	0.48	0.48	0.49	0.49	0.47	0.49	0.49	0.47	0.52
X_{An}	0.47	0.57	0.00	0.00	0.00	0.48	0.48	0.52	0.50	0.54	0.53	0.51	0.51	0.48	0.51	0.52	0.50	0.51	0.52	0.47

Table 5.2. Continued.

Sample	S26							17EG07													
Phase	Kfs	Kfs	Kfs	Kfs	Kfs	Kfs	Kfs	Pl	Pl	Pl	Pl	Pl	Pl	Pl	Pl	Pl	Pl	Pl	Pl	Pl	Kfs
Anal. no.	58	61	64	71	84	96	108	5	12	13	21	30	31	35	43	64	77	93	97	7
SiO_2	63.69	72.82	63.86	63.76	63.73	64.38	64.19	55.69	55.88	54.68	54.4	55.41	54.24	58.34	53.57	54.38	55.14	54.46	54.53	65.04
TiO_2	0.02	0.01	0.02	0.04		0.03	0.04	0.05	0.05	0.02	0.02	0.04		0.03		0.02	0.01	0.01	0.03	0.02
Al_2O_3	17.94	12.74	18.01	17.76	17.79	18.14	17.96	27.86	28.65	27.4	28.03	28.01	28.75	24.68	26.9	28.25	27.8	28.2	29.03	18.42
Cr_2O_3	0.31	1.17	0.13	0.08	0.08	0.05	0.01	0.4	0.6	0.05	0.12	0.04	0.15	0.22	0.05	0.13	0.19	0.14	0.2	0.21
FeO	0.31	1.17	0.13	0.08	0.08	0.05	0.01	0.4	0.6	0.05	0.12	0.04	0.15	0.22	0.05	0.13	0.19	0.14	0.2	0.21
MnO								0.01	0.03		0.01					0.01				0.01
MgO		0.46								0.02				0.04	0.02				0.01	
CaO								10.9	11.07	11.03	11.61	10.94	11.77	10.69	11.01	11.06	10.58	11.07	11.46	
ZnO			0.05	0.04	0.03			0.02	0.02	0.02		0.07		0.01	0.01	0.01	0.01	0.02	0.01	0.01
Na_2O	1.01	0.8	1.16	1.18	1.14	1.24	1.45	5.22	5.1	4.98	4.72	5.00	4.45	4.01	4.7	4.8	5.03	4.77	4.68	0.32
K_2O	14.1	9.62	13.83	13.88	13.62	13.6	13.46	0.29	0.28	0.34	0.23	0.27	0.33	0.18	0.31	0.33	0.34	0.24	0.26	14.98
P_2O_5	0.01		0.01			0.02		0.01	0.01	0.07	0.03	0.04	0.03	0.04	0.08	0.04	0.05	0.02	0.01	0.02
Total	97.39	98.79	97.2	96.82	96.47	97.51	97.12	100.85	102.29	98.66	99.29	99.86	99.87	98.46	96.7	99.16	99.34	99.07	100.42	99.24
O-basis	8	8	8	8	8	8	8	8	8	8	8	8	8	8	8	8	8	8	8	8
Si	3.014	3.301	3.017	3.022	3.027	3.021	3.022	2.503	2.483	2.501	2.477	2.500	2.457	2.650	2.499	2.477	2.504	2.481	2.456	3.022
Ti	0.001		0.001	0.001		0.001	0.001	0.002	0.002	0.001	0.001	0.001		0.001		0.001			0.001	0.001
Al	1.001	0.681	1.003	0.992	0.996	1.003	0.997	1.476	1.501	1.477	1.504	1.490	1.535	1.321	1.479	1.516	1.488	1.514	1.541	1.009
Fe^{2+}	0.012	0.044	0.005	0.003	0.003	0.002		0.015	0.022	0.002	0.005	0.002	0.006	0.008	0.002	0.005	0.007	0.005	0.008	0.008
Mn									0.001											
Mg		0.031								0.001				0.003	0.001				0.001	
Ca								0.525	0.527	0.541	0.566	0.529	0.571	0.520	0.550	0.540	0.515	0.540	0.553	
Zn			0.002	0.001	0.001			0.001	0.001	0.001		0.002						0.001		
Na	0.093	0.070	0.106	0.108	0.105	0.113	0.132	0.455	0.439	0.442	0.417	0.437	0.391	0.353	0.425	0.424	0.443	0.421	0.409	0.029
K	0.851	0.556	0.833	0.839	0.825	0.814	0.808	0.017	0.016	0.020	0.013	0.016	0.019	0.010	0.018	0.019	0.020	0.014	0.015	0.888
Cation	4.97	4.68	4.97	4.97	4.96	4.95	4.96	4.99	4.99	4.98	4.98	4.98	4.98	4.87	4.98	4.98	4.98	4.98	4.98	4.96
X_{Or}	0.90	0.89	0.89	0.89	0.89	0.88	0.86	0.02	0.02	0.02	0.01	0.02	0.02	0.01	0.02	0.02	0.02	0.01	0.02	0.97
X_{Ab}	0.10	0.11	0.11	0.11	0.11	0.12	0.14	0.46	0.45	0.44	0.42	0.45	0.40	0.40	0.43	0.43	0.45	0.43	0.42	0.03
X_{An}	0.00	0.00	0.00	0.00	0.00	0.00	0.00	0.53	0.54	0.54	0.57	0.54	0.58	0.59	0.55	0.55	0.53	0.55	0.57	0.00

Table 5.2. Continued.

Sample	17EG07			PLB7/2											PLB89A							
Phase	Kfs	Kfs	Kfs	Pl	Pl	Pl	Pl	Pl	Pl	Kfs	Kfs	Kfs	Kfs	Kfs	Pl	Pl	Pl	Pl	Pl	Pl	Kfs	
Anal. no.	22	29	92	18	19	37	50	51	35	36	39	52	54	16	17	20	26	56	58	22		
SiO_2	64.02	63.21	63.39	56.38	57.65	60.73	57.26	55.52	64.35	64.50	63.63	64.60	64.36	58.14	57.88	57.97	58.59	60.14	57.49	60.98		
TiO_2	0.01	0.03		0.01		0.03			0.01	0.04		0.04	0.05	0.04	0.02				0.68			
Al_2O_3	18.09	19.59	18.19	26.15	25.00	23.35	25.79	26.38	17.71	17.62	17.71	17.95	17.72	25.93	25.98	26.13	25.61	24.09	25.86	21.4		
Cr_2O_3	0.09	0.34	0.18	0.03	0.13	0.22	0.10	0.06	0.21	0.36	0.31	0.35	0.26	0.05	0.07	0.12	0.03	0.05	0.66	0.07		
FeO	0.09	0.34	0.18	0.03	0.13	0.22	0.1	0.06	0.21	0.36	0.31	0.35	0.26	0.05	0.07	0.12	0.03	0.05	0.66	0.07		
MnO			0.01						0.01	0.01	0.00	0.00	0.00	0.01	0.01					0.01		
MgO			0.01			0.01																
CaO				9.76	8.41	6.03	9.14	9.96						8.30	8.28	8.49	8.01	8.52	8.06	3.18		
ZnO	0.02	0.02	0.02	0.02		0.04		0.01	0.04	0.04		0.03	0.00		0.03			0.01		0.01		
Na_2O	0.4	0.41	0.31	6.06	6.68	7.84	6.37	5.64	0.77	0.69	0.72	0.88	1.32	6.53	6.45	6.49	6.74	6.42	6.72	2.68		
K_2O	14.74	14.3	14.73	0.20	0.12	0.16	0.17	0.19	14.42	14.57	14.63	13.99	13.78	0.13	0.18	0.15	0.26	0.11	0.15	11.82		
P_2O_5	0.02	0.01	0.03	0.07	0.03	0.05		0.03	0.01	0.05		0.04	0.02			0.02				0.04		
Total	97.48	98.25	97.05	98.71	98.15	98.68	98.93	97.85	97.74	98.24	97.31	98.23	97.77	99.18	98.97	99.49	99.27	99.39	100.28	100.26		
O-basis	8	8	8	8	8	8	8	8	8	8	8	8	8	8	8	8	8	8	8	8		
Si	3.023	2.968	3.011	2.568	2.633	2.740	2.599	2.552	3.032	3.031	3.028	3.026	3.028	2.620	2.615	2.609	2.637	2.698	2.591	2.812		
Ti		0.001								0.001		0.001	0.002	0.001	0.001				0.023			
Al	1.007	1.084	1.018	1.404	1.346	1.242	1.380	1.429	0.984	0.976	0.993	0.991	0.983	1.377	1.384	1.386	1.358	1.274	1.374	1.163		
Fe^{2+}	0.004	0.013	0.007	0.001	0.005	0.008	0.004	0.002	0.008	0.014	0.012	0.014	0.010	0.002	0.003	0.005	0.001	0.002	0.025	0.003		
Mn																						
Mg			0.001			0.001																
Ca				0.476	0.412	0.292	0.445	0.491						0.401	0.401	0.409	0.386	0.410	0.389	0.157		
Zn	0.001	0.001	0.001	0.001		0.001			0.001	0.001		0.001			0.001							
Na	0.037	0.037	0.029	0.535	0.592	0.686	0.561	0.503	0.070	0.063	0.066	0.080	0.120	0.571	0.565	0.566	0.588	0.558	0.587	0.240		
K	0.888	0.856	0.892	0.012	0.007	0.009	0.010	0.011	0.867	0.873	0.888	0.836	0.827	0.007	0.010	0.009	0.015	0.006	0.009	0.695		
Cation	4.96	4.96	4.96	5.00	4.99	4.98	5.00	4.99	4.96	4.96	4.99	4.95	4.97	4.98	4.98	4.98	4.99	4.95	5.00	5.07		
X_{Or}	0.96	0.96	0.97	0.01	0.01	0.01	0.01	0.01	0.92	0.93	0.93	0.91	0.87	0.01	0.01	0.01	0.02	0.01	0.01	0.64		
X_{Ab}	0.04	0.04	0.03	0.52	0.59	0.70	0.55	0.50	0.08	0.07	0.07	0.09	0.13	0.58	0.58	0.58	0.59	0.57	0.60	0.22		
X_{An}	0.00	0.00	0.00	0.47	0.41	0.30	0.44	0.49	0.00	0.00	0.00	0.00	0.00	0.41	0.41	0.42	0.39	0.42	0.40	0.14		

Table 5.2. Continued.

Sample	PLB89A								
Phase	Cpx	Cpx	Cpx	Cpx	Cpx	Cpx	Cpx	Cpx	Cpx
Anal no.	29	30	32	33	53	1	2	3	8
SiO_2	50.41	51.59	51.42	49.65	49.37	50.78	50.58	50.99	49.94
TiO_2	0.14	0.10	0.10	0.14	0.14	0.09	0.02	0.05	0.12
Al_2O_3	2.75	1.90	1.00	2.02	2.64	1.06	1.18	0.79	1.18
Cr_2O_3	0.01			0.02	0.01	0.04	0.04	0.01	
Fe_2O_3				3.50	3.50	2.94	3.49	2.77	4.04
FeO	16.26	14.54	14.71	12.22	13.34	11.81	11.78	11.82	10.72
MnO	0.16	0.14	0.17	0.13	0.12	0.16	0.22	0.19	0.16
MgO	9.53	9.3	9.76	9.57	10.02	10.51	10.58	10.48	10.67
CaO	19.47	21.67	21.71	21.64	20.1	22.33	22.14	22.67	22.08
Na_2O	0.31	0.29	0.32	0.39	0.39	0.32	0.26	0.28	0.35
K_2O	0.02	0.03		0.18	0.09		0.02		
P_2O_5		0.03	0.06		0.10	0.02	0.05	0.04	0.03
Total	99.06	99.59	99.25	99.46	99.82	100.06	100.36	100.10	99.30
O-basis	6	6	6	6	6	6	6	6	6
Si	1.954	1.987	1.988	1.918	1.902	1.942	1.932	1.951	1.924
Ti	0.004	0.003	0.003	0.004	0.004	0.003	0.001	0.002	0.003
Al	0.126	0.086	0.046	0.092	0.120	0.048	0.053	0.035	0.054
Cr				0.001		0.001	0.001		
Fe^{3+}				0.102	0.101	0.085	0.100	0.080	0.117
Fe^{2+}	0.530	0.470	0.480	0.395	0.430	0.378	0.376	0.378	0.345
Mn	0.005	0.005	0.006	0.004	0.004	0.005	0.007	0.006	0.005
Mg	0.551	0.534	0.562	0.551	0.575	0.599	0.602	0.597	0.613
Ca	0.809	0.894	0.899	0.896	0.830	0.915	0.906	0.929	0.911
Na	0.023	0.022	0.024	0.029	0.029	0.024	0.019	0.021	0.027
K	0.001	0.001	0.000	0.009	0.004		0.001		
Cation	4	4	4	4	4	4	4	4	4
X_{Mg}	0.51	0.53	0.54	0.58	0.57	0.61	0.62	0.61	0.64
X_{En}	0.29	0.28	0.29	0.30	0.31	0.32	0.32	0.31	0.33
X_{Fs}	0.29	0.26	0.25	0.21	0.23	0.20	0.20	0.20	0.18
X_{Wo}	0.42	0.46	0.46	0.49	0.45	0.48	0.48	0.49	0.49
X_{Jd}	0.03	0.04	0.03	0.01	0.02	0.01	0.01	0.01	0.01

Table 5.2. Continued.

Sample	PLB89A				
Phase	Hbl	Hbl	Hbl	Hbl	Hbl
Anal no.	4	5	6	7	10
SiO_2	42.51	41.13	41.40	40.58	40.49
TiO_2	1.78	1.94	1.73	2.07	1.96
Al_2O_3	10.60	11.02	10.96	11.26	10.97
Cr_2O_3	0.03	0.02	0.01	0.03	0.07
FeO	19.30	20.41	20.12	20.55	20.38
MnO	0.09	0.11	0.09	0.08	0.06
MgO	8.46	7.46	8.01	7.88	7.71
CaO	12.07	11.64	11.61	11.91	11.49
ZnO	0.02	0.00	0.01	0.03	0.14
Na2O	1.01	1.29	1.13	1.25	1.31
K_2O	1.34	1.49	1.54	1.60	1.51
P_2O_5	0.01	0.01	0.03	0.01	0.01
F	0.01	0.01	0.01	0.02	
H_2O	1.96	1.93	1.94	1.94	1.93
Total	99.21	98.46	98.59	99.18	98.05
O-basis	23	23	23	23	23
Si	6.485	6.375	6.370	6.247	6.292
Ti	0.205	0.227	0.200	0.239	0.229
Al	1.910	2.010	1.990	2.040	2.010
Cr	0.003	0.002	0.001	0.004	0.009
Fe^{3+}	0.205	0.234	0.405	0.366	0.416
Fe^{2+}	2.257	2.412	2.184	2.280	2.233
Mn	0.012	0.014	0.011	0.010	0.009
Mg	1.923	1.723	1.838	1.808	1.786
Ca	1.974	1.933	1.913	1.964	1.914
Zn	0.003	0.000	0.001	0.003	0.017
Na	0.299	0.387	0.337	0.373	0.396
K	0.260	0.295	0.302	0.314	0.299
Cation	15.54	15.61	15.55	15.65	15.61
OH*	2.00	1.99	1.99	1.99	2.00
F	0.00	0.01	0.01	0.01	0.00
X_{Mg}	0.46	0.42	0.46	0.44	0.44

Table 5.3. Results of conventional geothermobarometry from representative samples of charnockite.

Sample No.	Thermo/barometer used	Model	Assumed P/T	Results
S26	GOPQ-RCLC	Pattison et al. (2003)		827°C, 9.03 kbar
	Gt-Opx thermometer	Lee and Ganguly,(1988)	8.0 kbar	722 °C
	Gt-Ilm thermometer	Pownceby et al. (1987)		639°C
PLB2B	GOPQ-RCLC	Pattison et al. (2003)		741°C , 7.50 kbar
	Gt-Opx thermometer	Lee and Ganguly,(1988)	8.0 kbar	781°C
	Opx-Ilm thermometer	Bishop (1980)	8.0 kbar	756°C
	Gt-Ilm thermometer	Pownceby et al. (1987)		563°C
	Ti in Bt thermometer	Henry et al. (2005)		770°C
	Gt-Bt thermometer	Ganguly et al. (1996)	8.0 kbar	572°C
PLB7_2	Gt-Ilm thermometer	Pownceby et al. (1987)		545°C
	Gt-Bt thermometer	Ganguly et al. (1996)		612°C
	Ti in Bt thermometer	Henry et al. (2005)		766°C
17EG18B	GOPQ,RCLC	Pattison et al. (2003)		910°C, 8.92 kbar
	Gt-Opx thermometer	Lee and Ganguly,(1988)	8.0 kbar	790°C
	Gt-Bt thermometer	Ganguly et al. (1996)		453°C
	Ti in Bt thermometer	Henry et al. (2005)		831°C
17EG07	GOPQ,RCLC	Pattison et al. (2003)		784°C, 7.30 kbar
	Gt-Bt thermometer	Ganguly et al. (1996)		422 °C
	Ti in Bt thermometer	Henry et al. (2005)		799°C
	Gt-Ilm thermometer	Pownceby et al. (1987)		672°C
PLB89A	Gt-Bt thermometer	Ganguly et al. (1996)		781°C
	Ti in Bt thermometer	Henry et al. (2005)		756°C
	Gt-Ilm thermometer	Pownceby et al. (1987)		596°C
	Gt-Cpx thermometer	Ganguly (1979)	8.0 kbar	823°C

Table 5.4. Whole rock data of representative charnockite samples.

Sample	17EG18B	17EG10	PH12	PLB24	PLB2b	17EG13	17EG12	17EG17	PLB7/2	S 26	19EG06	PLB71B	PLB82A	PLB89A
SiO_2	53.9	62.09	59.72	60.13	54.76	64.31	66.00	69.15	69.80	64.11	63.41	70.21	72.13	63.16
TiO_2	0.64	1.34	1.03	1.66	1.95	1.1	0.99	0.65	0.95	1.4	0.95	1.06	0.41	1.42
Al_2O_3	14.77	14.84	15.43	15.00	18.51	13.33	14.77	14.86	12.06	14.33	15.46	13.84	13.23	14.2
FeO	9.96	7.56	6.35	9.95	7.73	7.57	5.76	3.96	5.84	6.3	5.59	4.02	2.76	6.96
Fe2O3	1.23	0.93	0.78	1.23	0.95	0.94	0.71	0.49	0.72	0.78	0.69	0.5	0.34	0.86
Mno	0.12	0.11	0.09	0.17	0.09	0.14	0.06	0.05	0.07	0.1	0.08	0.05	0.05	0.11
MgO	8.35	2.16	2.58	4.08	5.07	1.94	0.79	0.68	1.07	1.82	1.68	1.73	0.56	4.31
CaO	5.36	3.78	4.94	5.64	5.8	3.61	3.21	2.94	2.97	3.42	4.32	4.26	2.81	4.95
Na_2O	2.01	2.12	2.06	2.49	1.88	2.22	1.64	2.23	2.11	1.71	2.11	1.89	2.56	2.46
K_2O	1.86	3.61	3.93	1.36	4.13	3.1	5.14	5.02	3.06	4.49	4.19	2.23	3.74	1.97
P_2O_5	0.34	0.48	0.27	0.38	0.54	0.48	0.32	0.2	0.19	0.34	0.41	0.04	0.12	0.4
Total	98.54	99.02	97.18	102.09	101.41	98.74	99.39	100.23	98.84	98.8	98.89	99.83	98.71	100.81
(in ppm)														
Cr	726	42	35	39	61	55	29	19	28	34	88	48	13	44
Ni	54	18	9	0	17	11	4	4	7	8	20	28	8	10
Cu	10	11	10	24	27	7	20	12	20	7	16	35	5	21
Zn	211	122	108	123	88	124	73	61	77	120	74	97	44	99
Ba	599	697	786	249	1955	808	1116	626	470	1005	1616	1188	466	600
Be	6	2	5	3	3	2	<1	<1	2	1	*bdl*	*bdl*	*bdl*	*bdl*
Co	81.5	102.9	82.6	81.3	76.2	112.1	120.8	126.2	132.6	125	*bdl*	*bdl*	*bdl*	*bdl*
Cs	4.5	0.3	3.8	0.3	2.8	0.2	0.1	0.2	0.9	0.1	*bdl*	*bdl*	*bdl*	*bdl*
Ga	19.3	20.3	18.5	19.3	23.1	18.9	18	17.1	16.9	16.8	16	16	11	18
Hf	4	11.1	7	6.9	14.2	10.6	9.3	6.7	9.8	13	*bdl*	*bdl*	*bdl*	*bdl*
Nb	25.2	26.4	15	22.3	24.3	20	22.2	17.2	19.8	41.9	*bdl*	*bdl*	*bdl*	*bdl*
Rb	116	147.1	178.8	39.4	179.4	111.1	168.7	182.9	154.6	128.4	220	62	247	170
Sn	1	<1	<1	<1	<1	<1	<1	<1	<1	<1	*bdl*	*bdl*	*bdl*	*bdl*
Sr	168	106	129.9	108.8	222.9	145.1	155.2	121.9	85.2	129.3	285	164	57	109
Ta	2.4	1.7	2	1.8	1.9	1.3	3	3.2	3.1	3.8	*bdl*	*bdl*	*bdl*	*bdl*
Th	41.1	16.5	10.6	3	16.1	6.4	9.8	10.6	54.1	74	*bdl*	*bdl*	*bdl*	*bdl*
U	4.8	1.1	1.7	0.8	1.4	0.5	0.5	0.6	2.7	1.2	*bdl*	*bdl*	*bdl*	*bdl*
V	161	106	89	111	219	75	68	44	64	73	83	105	35	109
W	435.2	691	524.2	444.1	421.2	839.8	871.4	907.5	961.8	942.7	*bdl*	*bdl*	*bdl*	*bdl*
Zr	158.5	404.2	255.2	261.9	502.3	390.4	329.3	237	350.9	497.3	235	257	84	307
Y	29.6	79.3	18.4	36.9	43.7	82.3	39	26.9	34.3	71.4	9	8	7	29
La	107	81.5	41.6	39.4	61.7	55.8	65.7	61.4	75	126.5	102	23	58	127
Ce	193	165.3	84.3	82.3	131.9	108	124.9	119.3	147.2	258.1	169	90	96	182
Pr	21.82	19.67	9.91	10.25	15.99	13.23	15.13	14.21	17.84	30.18	*bdl*	*bdl*	*bdl*	*bdl*
Nd	75.1	73.6	36.5	42.1	62	51.2	55.8	49.8	63.7	109.1	*bdl*	*bdl*	*bdl*	*bdl*
Sm	11.02	12.85	6.22	8.14	12.44	10.42	10.16	9.62	10.97	17.59	9	3	9	13
Eu	1.37	1.92	1.55	1.79	3.13	1.81	2.33	1.72	1.35	2.53	*bdl*	*bdl*	*bdl*	*bdl*
Gd	8.07	11.53	5.2	7.93	12.29	11.51	9.35	8.27	9.07	14.22	*bdl*	*bdl*	*bdl*	*bdl*
Tb	1.1	1.98	0.75	1.17	1.78	2.16	1.32	1.16	1.26	2.21	*bdl*	*bdl*	*bdl*	*bdl*
Dy	6	13.92	3.94	7.1	9.73	14.86	7.73	6.14	7	13.11	*bdl*	*bdl*	*bdl*	*bdl*
Ho	1.03	3.06	0.74	1.37	1.65	3.2	1.5	1	1.38	2.74	*bdl*	*bdl*	*bdl*	*bdl*
Er	3.05	9.45	1.98	4.15	3.65	9.64	4.43	2.48	3.53	8.15	*bdl*	*bdl*	*bdl*	*bdl*
Tm	0.4	1.35	0.25	0.61	0.38	1.31	0.6	0.31	0.45	1.12	*bdl*	*bdl*	*bdl*	*bdl*
Yb	2.59	8.55	1.48	4.07	2.23	8.45	3.81	1.9	2.66	7.27	*bdl*	*bdl*	*bdl*	*bdl*
Lu	0.38	1.26	0.2	0.63	0.3	1.26	0.57	0.27	0.38	1.07	*bdl*	*bdl*	*bdl*	*bdl*
ΣREE	432	406	195	211	319	293	303	278	342	594	280	116	163	322
Mg#	60	34	42	42	54	31	20	23	25	34	35	43	27	52
Normative values														
Quartz	4.63	20.92	15.03	16.59	4.84	24.99	25.78	27.54	34.43	23.89	20.73	36.67	34.49	20.90
Albite	17.01	17.94	17.43	21.07	15.91	18.78	13.88	18.87	17.85	14.47	17.85	15.99	21.66	20.82
Orthoclase	10.99	21.33	23.22	8.04	24.41	18.32	30.38	29.67	18.08	26.53	24.76	13.18	22.10	11.64
Anorthite	24.37	15.62	21.25	25.50	25.25	14.77	13.83	13.28	13.49	14.75	18.75	20.87	13.16	21.88
Hypersthene	37.24	16.49	15.28	24.99	22.99	16.40	10.44	7.58	11.36	13.33	12.46	9.62	5.60	20.64
Apatite	0.79	1.11	0.63	0.88	1.25	1.11	0.74	0.46	0.44	0.79	0.95	0.09	0.28	0.93
Diopside	0.00	0.00	1.25	0.00	0.00	0.00	0.00	0.00	0.00	0.00	0.00	0.00	0.00	0.05
Ilmenite	1.22	2.54	1.96	3.15	3.70	2.09	1.88	1.23	1.80	2.66	1.80	2.01	0.78	2.70
Corundum	0.52	1.72	0.00	0.09	1.69	0.91	1.44	0.89	0.33	1.25	0.58	0.67	0.15	0.00
Magnetite	1.78	1.35	1.13	1.78	1.38	1.36	1.03	0.71	1.04	1.13	1.00	0.72	0.49	1.25

bdl - below detection limit

Table 5.5 Trace element and REE data of zircon spots from representative samples of charnockite (values in ppm).

Spot no.	Domain	Ti	Y	Nb	La	Ce	Pr	Nd	Sm	Eu	Gd	Tb	Dy	Ho	Er	Tm	Yb	Lu	Hf
Sample 17EG07																			
2	Osc	28.67	159.92	2.44	1.61	13.35	1.98	14.39	14.84	0.86	20.00	4.27	28.38	5.75	12.27	2.04	14.17	2.04	13617.09
8	Osc	14.28	1226.13	2.54	0.82	7.36	1.01	5.44	6.37	0.40	43.38	15.53	149.05	45.46	163.47	27.27	220.65	37.72	12280.86
13	Osc	14.91	174.26	1.26	0.30	7.33	0.52	8.81	6.56	0.31	22.14	3.35	27.83	5.39	14.89	2.14	13.59	2.11	12479.02
12	Ov	2.67	685.83	2.06	0.00	15.59	0.10	1.71	4.40	0.69	23.75	6.12	73.21	22.60	91.67	18.51	157.04	30.47	10349.26
Sample 17EG10																			
2	Osc	3.54	600.50	1.46	2.48	37.66	1.66	11.87	8.62	2.66	20.90	6.23	69.60	20.10	82.63	15.23	117.86	22.03	11409.29
3	Osc	25.40	908.37	1.49	2.80	29.72	2.78	18.17	7.89	2.44	21.80	6.80	94.32	31.05	129.20	23.19	195.69	35.04	11028.38
16	Osc	2.77	1851.59	3.21	3.82	26.10	1.91	11.16	6.74	1.10	27.46	12.15	155.40	57.88	270.80	55.18	458.98	94.72	11619.25
17	Osc	2.46	1450.67	1.48	0.58	11.07	1.19	6.83	10.00	1.35	42.39	13.03	155.68	49.83	203.14	38.21	315.21	60.21	10899.70
20	Osc	25.68	1283.37	2.40	4.00	42.27	3.25	22.64	9.70	2.09	41.23	11.52	123.90	41.23	194.84	35.21	303.86	59.82	10257.37
6	Ov	33.08	734.01	1.75	0.74	7.59	0.68	5.53	5.27	0.57	29.94	9.75	79.85	21.92	85.27	15.11	124.93	22.06	11108.64
Sample 17EG17																			
1	Osc	24.13	1242.52	2.35	0.79	7.89	1.27	13.24	19.04	1.53	73.30	17.60	163.39	40.16	130.33	20.10	140.80	22.36	11150.23
5	Osc	8.69	363.30	1.84	0.22	3.37	0.38	2.53	3.08	0.02	17.87	4.52	40.27	11.62	42.28	6.89	61.02	9.84	11729.12
6	Osc	14.33	1179.03	3.51	0.33	9.37	0.88	4.97	6.21	1.30	21.33	8.97	111.94	39.47	189.80	34.94	311.94	61.18	11297.57
10	Osc	3.70	1003.53	1.59	0.00	1.58	0.02	0.76	2.06	0.02	12.85	6.53	85.65	33.10	178.67	35.36	334.51	59.87	11816.70
12	Osc	19.16	716.83	1.35	2.80	12.49	2.23	15.80	9.42	2.06	24.29	9.02	86.13	23.55	82.60	12.69	115.63	18.53	12266.06
14	Osc	30.34	2235.87	3.52	1.12	11.68	0.95	8.23	10.56	1.01	59.40	19.74	225.82	78.09	366.13	66.25	571.79	97.70	10477.62
16	Osc	4.58	784.96	2.38	6.09	33.32	4.82	29.39	15.25	4.10	32.81	8.25	82.47	26.77	119.56	22.81	187.70	34.77	9980.62
20	Osc	19.70	2056.24	1.82	0.01	4.53	0.37	5.30	10.68	0.30	51.93	17.52	208.96	72.26	319.62	59.19	527.50	91.75	10102.69
3	Ov	13.52	702.55	1.72	0.14	3.02	0.33	2.54	4.87	0.12	27.26	8.58	85.07	21.95	71.28	11.50	83.01	14.35	11447.96
7	Ov	14.56	1368.01	3.91	6.36	32.36	3.16	20.11	8.79	4.39	26.35	8.20	120.24	44.11	212.88	47.62	448.83	86.35	13156.58
9	Pa	18.76	3991.34	2.80	3.18	12.18	1.12	6.63	8.84	0.28	58.53	27.23	372.36	134.31	621.59	114.88	959.68	169.13	10154.84
13	Ov	8.35	119.60	0.78	0.10	2.89	0.16	2.66	4.34	0.48	16.53	2.96	18.68	4.00	9.57	1.52	10.54	1.85	12283.84
Sample 19EG06																			
2A	Osc	24.82	642.94	2.56	2.74	21.92	1.36	9.20	5.60	2.18	19.59	5.11	60.79	21.74	97.63	18.77	164.32	32.75	10076.41
5	Osc	15.91	1496.56	2.57	4.12	12.64	1.32	5.48	4.56	1.66	20.61	8.14	123.63	51.75	263.34	55.43	565.66	110.95	11709.19
6B	Osc	0.06	2690.35	3.23	3.23	6.73	0.87	3.94	2.09	1.35	26.73	11.47	198.35	84.78	491.36	117.37	1187.72	239.31	12306.09
9	Osc	3.21	1755.20	3.25	1.00	4.01	0.25	3.07	2.64	0.34	19.47	9.73	152.78	61.97	331.98	72.97	705.61	135.94	12299.98
11A	Osc	4.05	3590.45	3.86	4.27	12.08	1.43	7.60	4.03	2.93	31.36	17.08	275.76	109.30	566.18	133.91	1216.43	217.73	13052.79
8	XC	82.18	404.98	2.23	0.00	3.36	0.02	0.44	1.26	0.08	10.38	3.08	40.03	12.92	72.53	12.97	121.12	22.25	8477.28
10	XC	8.35	1236.35	1.99	0.15	3.31	0.13	0.75	4.50	0.10	22.39	9.63	116.36	41.98	210.20	39.34	352.76	63.76	11012.38
4	Pa	16.56	471.72	1.85	0.00	11.38	0.05	0.84	2.11	0.24	14.00	3.62	46.50	15.13	73.34	13.76	122.81	24.04	11097.39
Sample PH9A																			
1	Osc	12.56	571.19	0.99	24.94	76.87	9.61	40.33	8.38	0.24	20.01	5.42	58.62	17.55	86.33	17.64	150.93	31.17	9157.93
2	Osc	3.26	525.09	1.68	0.09	5.57	0.17	1.21	1.42	0.11	8.66	2.48	41.39	14.07	74.59	17.54	161.32	32.92	11407.70
3	Osc	2.48	986.68	3.52	0.15	9.08	0.14	2.32	4.86	0.14	20.56	7.67	89.80	31.31	153.60	30.26	259.98	50.58	9968.42
4	Osc	3.34	631.84	1.68	8.29	29.91	2.57	16.80	5.23	0.02	12.61	4.20	61.49	19.43	98.97	19.05	164.11	31.14	8833.77
5	Osc	3.94	700.84	1.42	0.50	8.13	0.34	1.73	2.18	0.02	13.84	4.64	59.84	23.25	111.74	22.50	179.83	36.74	9288.86
7	Osc	5.09	701.24	1.71	1.73	10.03	0.60	2.77	2.01	0.03	11.82	5.61	64.31	22.14	106.77	22.27	183.69	33.10	9689.20
8	Osc	0.00	694.37	1.41	0.38	8.74	0.42	1.81	3.51	0.09	14.21	5.74	60.43	22.39	103.41	20.81	166.85	32.83	8797.17
11	Osc	2.42	594.09	2.32	0.20	8.33	0.21	1.34	1.46	0.03	8.21	3.09	48.41	16.75	87.36	19.68	179.24	38.65	10764.23
12	Osc	2.79	720.77	1.30	0.14	5.59	0.03	1.01	1.67	0.15	16.89	5.35	65.44	24.39	116.50	21.86	195.27	36.29	9208.35
13	Osc	2.70	689.42	2.47	0.03	5.09	0.12	0.44	1.61	0.02	14.48	4.38	63.45	22.72	100.17	20.42	184.84	36.88	9298.96
14	Osc	5.90	800.67	2.34	1.64	18.59	1.70	12.31	3.95	0.22	17.20	6.13	70.63	24.45	126.50	26.21	222.49	43.34	10224.53
16	Osc	3.55	656.30	1.13	0.00	3.99	0.00	0.37	1.63	0.05	10.48	4.33	57.80	21.53	96.20	21.08	184.29	31.89	8819.41
Sample PLB71B																			
1	Osc	0.00	776.26	1.01	0.02	5.41	0.07	1.12	2.21	0.06	17.76	5.67	74.34	25.14	107.59	21.64	185.12	34.16	12418.15
3	Osc	11.19	782.92	1.26	0.00	2.56	0.00	2.61	2.01	0.43	32.40	8.66	87.53	24.04	89.56	15.78	131.76	21.83	15600.89
4	Osc	6.90	1326.08	5.19	1.27	15.40	0.63	6.21	5.69	0.90	29.50	9.82	111.23	43.09	194.27	43.11	364.73	67.65	13742.72
5	Osc	0.00	1737.00	1.64	0.04	1.31	0.11	1.95	2.45	0.06	31.33	11.64	144.06	56.24	240.17	48.81	441.49	78.24	11104.88
6	Osc	0.00	1393.18	1.52	0.00	4.01	0.23	2.85	6.97	0.17	38.91	11.49	143.49	46.11	185.98	37.62	326.66	56.73	12532.11
7	Osc	7.50	974.43	1.13	0.00	2.53	0.41	0.38	2.01	0.11	22.58	8.84	88.18	29.05	113.65	21.72	164.14	28.40	13984.25
8	Osc	0.00	1248.44	0.54	0.00	2.29	0.33	0.53	3.41	0.50	30.34	12.59	134.28	37.78	126.77	20.89	169.48	26.47	12142.07
9	Osc	5.47	2506.69	2.62	1.69	13.62	0.92	8.12	9.47	0.79	39.33	16.76	217.44	78.44	347.55	69.52	608.27	107.52	11444.40
11	Osc	2.16	2013.78	1.79	2.13	17.82	1.78	7.18	6.33	2.69	46.63	16.23	192.25	73.60	333.33	63.04	561.84	100.11	10526.60
12	Osc	0.00	970.27	0.66	0.08	2.48	0.09	0.81	1.64	0.24	21.34	7.92	100.24	30.27	118.37	21.24	162.23	25.46	12287.44
13	Osc	5.04	495.37	0.65	0.01	5.65	0.00	0.00	1.03	0.05	11.18	4.10	48.35	16.22	70.19	13.75	116.60	20.54	10261.31
15	Ov	0.00	3201.89	2.80	0.76	11.88	1.42	13.14	16.64	0.83	93.72	29.84	340.71	114.18	473.59	87.20	680.62	124.36	9448.76
Sample PLB82A																			
1A	Osc	2.68	3995.99	9.38	7.69	37.32	3.11	18.81	12.21	0.27	46.13	22.45	305.79	124.61	668.30	146.67	1381.30	286.45	14453.42
2B	Osc	3.06	1301.70	2.33	8.16	36.91	7.73	35.46	19.67	0.73	25.31	9.54	123.82	47.80	218.29	48.37	474.60	94.02	13700.24
Sample PLB89A																			
4	Osc	9.94	1647.68	1.64	1.57	13.74	1.02	5.98	5.64	0.25	35.40	11.69	150.67	55.48	258.41	50.05	428.29	81.10	11328.17
5	Osc	0.29	991.65	2.89	4.47	31.34	3.60	20.47	18.00	2.69	34.06	10.31	94.22	30.95	160.83	32.03	288.18	59.75	10508.08
6B	Osc	1.99	1094.19	4.82	6.00	24.57	3.11	18.00	5.19	0.05	18.33	7.40	87.97	35.96	182.06	36.31	340.47	69.13	12775.76
11	Osc	3.27	1653.19	1.69	0.68	9.02	0.29	2.87	2.95	0.08	28.86	10.44	146.48	54.99	255.98	51.37	441.94	88.66	12700.64
12	Osc	6.51	1310.55	5.47	1.28	14.97	0.82	6.03	5.01	0.06	22.05	8.33	114.98	43.85	214.18	43.10	382.88	78.63	12207.37
13	Osc	4.86	2226.99	3.22	8.56	39.05	4.71	26.38	22.75	1.71	67.53	17.42	208.78	72.85	346.96	69.06	626.60	131.07	11825.63
15	Osc	2.67	1464.37	0.93	2.22	13.54	1.05	4.43	8.07	0.40	32.53	11.00	130.24	49.48	239.71	43.36	396.70	75.28	12001.49
1	Pa	8.65	2233.58	2.49	3.99	24.97	2.56	17.74	17.78	1.10	53.40	15.89	197.45	72.82	357.63	72.52	640.10	128.31	11630.18
3	Ov	2.11	1690.35	3.77	5.78	26.58	3.40	23.03	16.69	1.63	51.95	14.61	156.22	59.59	249.06	49.99	454.66	93.17	10820.24

Osc- Oscillatory zoned domain, Ov- Overgrowth domain, Pa-Patchy domain, XC- Xenocrystic core

Table 5.6. Whole rock data of representative Granite samples.

Sample	17EG09	17EG15	PLB79	PLB2	PH10
SiO2	69.4	71.3	56.7	72.9	75.6
TiO2	0.34	0.75	1.18	0.09	0.49
Al2O3	13.95	13.95	18.35	15.3	12.6
Cr2O3	0.00	0.00	0.01	0.00	0.00
MnO	0.04	0.08	0.10	0.01	0.10
FeO	4.03	5.71	7.96	0.99	5.21
Fe2O3	3.59	5.08	7.08	0.88	4.64
CaO	0.53	2.00	3.68	2.42	1.48
MgO	1.48	1.00	1.90	0.07	0.68
Na2O	1.16	1.15	2.66	4.06	1.28
K2O	7.66	4.86	4.77	3.46	3.74
P2O5	0.24	0.18	0.33	0.03	0.05
SrO	0.02	0.02	0.02	<0.01	0.01
BaO	0.08	0.1	0.12	0.03	0.09
LOI	0.16	0.09	0.55	0.05	0.02
Total	98.65	100.56	97.45	99.3	100.78
Ag	<0.5	<0.5	<0.5	<0.5	<0.5
As	<5	<5	55	<5	<5
Cd	<0.5	<0.5	<0.5	<0.5	<0.5
Co	7	9	13	<1	9
Cu	6	4	8	4	11
Li	10	50	80	40	30
Mo	1	<1	<1	<1	1
Ni	14	10	16	2	13
Pb	72	47	53	41	40
Sc	11	10	16	2	11
Tl	<10	<10	<10	<10	<10
Zn	35	66	106	19	63
Ba	710	918	1105	241	804
Ce	265	151.5	104.5	55.8	55.6
Cr	9	33	48	6	33
Cs	0.16	4.4	104.5	1.57	3.46
Dy	19.4	6.36	8.72	2.78	13.2
Er	10.5	2.64	4.27	1.02	9.35
Eu	1.7	1.66	1.81	0.84	1.76
Ga	13.9	20.1	25.6	21.2	14.9
Gd	21.7	9.36	10.5	4.05	7.23
Hf	6.95	8.86	10.35	3.72	14.75
Ho	3.82	1.12	1.53	0.45	3.02
La	119	71.5	49.2	27.1	30.4
Lu	1.09	0.31	0.55	0.1	1.14
Nb	9.53	21.7	33.2	2.99	12.2
Nd	112	60.6	45.7	22.6	20.5
Pr	30.3	16.9	12.05	6.14	5.83
Rb	360	319	399	218	179.5
Sm	21.7	10.95	9.19	4.22	4.26
Sn	<0.5	2.4	20.2	2.5	1.5
Sr	131.5	146	168	39.3	69.1
Ta	0.1	1.8	4.5	<0.1	0.9
Tb	3.31	1.26	1.62	0.54	1.66
Th	91.9	39.7	17.2	9.15	12.45
Tm	1.31	0.36	0.56	0.12	1.3
U	6.13	4.02	5.12	0.77	2.4
V	22	54	113	<5	52
W	<0.5	0.6	10.8	<0.5	1.3
Y	110	30.9	44.9	11.8	88.4
Yb	8.22	2.16	3.61	0.67	8.32
Zr	260	333	400	128	553
Eu/Eu*	0.17	0.35	0.38	0.43	0.62
Quartz	28.88	38.38	10.00	30.41	47.47
Corrundum	3.36	3.59	2.91	0.55	3.88
Orthoclase	45.27	28.72	28.19	20.45	22.10
Albite	9.82	9.73	22.51	34.36	10.83
Anorthite	1.06	8.75	16.10	11.81	7.02
Hypersthene	7.64	7.69	11.73	1.13	6.81
Magnetite	5.21	7.37	10.27	1.28	6.73
Ilmenite	0.65	1.43	2.24	0.17	0.93
Apatite	0.57	0.43	0.78	0.07	0.12